# CARDIOVASCULAR MAGNETIC RESONANCE IMAGING FOR IN VIVO ASSESSMENT OF THE AGE OF MYOCARDIAL INFARCT AND FOR IDENTIFICATION OF SIGNIFACT CORONARY HEART DISEASE IN PATIENTS WITH PERIPHERAL ARTERIAL DISEASE

**Ph.D. Thesis by:**

**Robert Kirschner, M.D.**

Head of the Doctoral School: Prof. Sámuel Komoly MD, DSc

Head of the Doctoral Program: Prof. Erzsébet Rőth MD, DSc

Supervisor: Prof. Tamás Simor MD, PhD

Heart Institute

University of Pécs, Pécs, Hungary

2011

## Contents

# ABBREVIATIONS

| | |
|---|---|
| CA | contrast agent |
| CMR | cardiovascular magnetic resonance |
| DE MRI | delayed enhancement MRI |
| DSMRI | dobutamine stress MRI |
| FOV | field of view |
| Gd(ABE-DTTA) | gadolinium (*N*-(2-butyryloxyethyl)-*N*¢-(2-ethyloxyethyl)-*N*,*N*¢-bis[*N*¢¢,*N*¢¢-bis(carboxymethyl)acetamido]-1,2-ethanediamine |
| Gd(DTPA) | gadolinium diethlynetriamine penta-acetic acid |
| IR | inversion recovery |
| LAD | left anterior descending coronary artery |
| LE MRI | late enhancement MRI |
| MRI | magnetic resonance imaging |
| R1 | longitudinal relaxation rate |
| ROI | region of interest |
| SI | signal intensity |
| SIE | signal intensity enhancement |

| | |
|---|---|
| T1 | longitudinal relaxation time |
| T2 | transverse relaxation time |
| TI | inversion time |

# 1 INTRODUCTION

## 1.1 Ischemic Heart Disease and Development of Diagnostic Imaging

Ischemic heart disease remains the leading cause of death in the Western world, and myocardial infarction is a key component of the burden of cardiovascular disease [1]. Efforts for the decrease of the incidence and case fatality of myocardial infarction are important determinants of the desired decline in coronary disease mortality. One of the key elements of these efforts could be the better recognition of pathological processes of different tissues following myocardial infarct. Medical, surgical or interventional treatment needs to be tailored for each individual patient based on the ongoing pathological processes. This requires accurate and quantitative assessment of the underlying pathology. The development of different imaging modalities could lead to better in vivo assessment of the irreversibly injured myocardial tissue as well as of the ongoing pathological processes during the healing of myocardial scar following myocardial infarct. This may contribute to the progress in the research field of scar tissue evolution process. The progress of this research area may supply the intervention to the scar tissue evolution processes, which could lead to better quality of treatment and better outcome for patients following myocardial infarct.

Another important aspect for the decline of the mortality of cardiovascular disease could be the identification of patients without symptoms but having the highest risk for cardiovascular mortality. Peripheral arterial disease (PAD) is a significant epidemiological problem by which 60.000 percutane angioplasty (PTA) and 100.000 amputations are implemented annually in the USA [2]. Due to the systemic nature of the atherosclerosis and because of the typical existence of multiplex lesions, patients with peripheral arterial disease often have coronary heart disease,

as well. Therefore, the risk of coronary events is high. Most of the patients with PAD dies in consequence of his/her coronary artery disease [3]. Also very serious coronary artery disease can remain often asymptomatic because of the physical disability of the patient with PAD. The cardiology assessment of patients with PAD would be of great importance even if they do not have cardiac symptoms. Medical, surgical or interventional treatment for each identified patient being at high risk for undesirable cardiovascular events is warranted to decrease coronary disease mortality in this subgroup of patients.

### 1.2 MRI – Imaging Modality for in Vivo Assessment of Tissue Pathology

Magnetic Resonance Imaging (MRI) is a unique, high resolution, noninvasive imaging technique which came into clinical use in the early 1980s. Unlike x-rays, radioisotope studies, and even computed tomography (CT) studies, it does not rely on radiation. Instead, it is based on the principles of nuclear magnetic resonance (NMR) spectroscopy. Images are generated by spatially encoding the NMR signal coming from nuclei (eg. protons) present in the object [4]. The NMR signals are induced by the application of time-varying linear magnetic field gradients [5]. In the course of the most commonly used $^{1}H$ MRI, radio waves are directed at protons, the nuclei of hydrogen atoms, in a strong magnetic field. The protons are first “excited” and then “relaxed”, causing them to emit radio signals that can be processed by computer to form an image. In the body, protons are most abundant in hydrogen atoms of water. $^{1}H$ MRI shows differences in the water content and distribution in various body tissues, therefore this imaging modality is currently the closest to the above mentioned desired need to assess different soft tissues and pathological processes in vivo. It involves that detailed comprehension of pathophysiology of

myocardial infarction is inevitable for the interpretation of cardiac MRI images following myocardial infarction.

### 1.2.1 Pathophysiology of Myocardial Infarction

The coronary artery is vulnerable to atherosclerosis, which is the main cause of ischemic heart disease. The cause of acute myocardial infarction is usually the thrombotic occlusion of an epicardial coronary artery [6]. The duration of myocardial ischemia determines whether an episode of vascular occlusion leads to reversible or irreversible myocardial injury. After the onset of insufficient myocardial oxygenation, it takes several hours before larger amounts of cell death occur and myocardial necrosis can be identified by macroscopic or microscopic post-mortem examination. Complete necrosis of all myocardial cells within the area at risk requires at least 2–4 h or longer depending on the presence of collateral circulation to the ischemic zone, persistent or intermittent coronary arterial occlusion, the sensitivity of the myocytes to ischemia, pre-conditioning, and/or, finally, individual demand for myocardial oxygen and nutrients [7]. Within 10 seconds after occlusion of the coronary artery, the myocardium initiates anaerobic glycolysis, followed by the accumulation of lactate and other metabolites [8]. Acute myocardial infarction begins in the subendocardium within 20–40 minutes after occlusion of the coronary artery and spreads toward the subepicardium. This concept of infarct progression has been termed the wavefront of myocardial necrosis [9, 10]. In histology level [11], nuclear shrinkage and loss, as well as cytoplasmatic eosinophylia are seen initially. Interstitial edema, hemorrhage, contraction band necrosis and leukocyte infiltration can be observed within the first 4 days, which is called acute inflammatory response. Contraction band necrosis is characterized by hypercontracted myofibrils and contraction bands and mitochondrial damage, caused by calcium influx into dying cells resulting in arrest of the cells in the contracted state. This phase is

followed by granulation tissue formation that manifests itself by penetration of blood capillaries and connective tissue from the periphery.

In terms of clinical therapy it is essential that the diagnosis of an acute coronary syndrome should be established quickly and accurately as therapy has to be instigated to limit myocardial necrosis [7]. Additional myocardial cell death may occur from reperfusion after prolonged ischemia (reperfusion injury) [12]. During ischemia, a large portion of the area at risk undergoes biochemical and pathological changes, associated with anoxia but remains potentially viable. At reperfusion, the potentially viable cells may reverse the changes occurring during ischemia and recover normal function or progress to necrosis. Without intervention, in the first four days, the size of the infarct region may expand. Until the third week, muscle fibers are removed (subacute infarct) and then replaced by collagen formation in the following weeks (fully mature scar). It is followed by a long process of scar maturation and the remodeling of the myocardium, which takes several months.

Reperfusion of ischemic myocardium can be implemented by either iv. fibrinolysis, percutaneous coronary intervention (PCI) or coronary artery bypass grafting (CABG). Even after restoration of the flow in the occluded coronary artery, expansion of infarction and progression of microvascular obstruction may occur [10, 13, 14]. Postischemic reperfusion intensifies the development of interstitial or intracellular edema in the injured areas [15-17]. Intramyocardial hemorrhage is a common type of reperfusion injury. It is more common in reperfused infarcts (it takes about 33-38% of all cases) than in non-reperfused ones. Hemorrhage is disadvantageous for the potential recovery of left ventricular function following reperfusion therapy of myocardial infarct [18, 19]. Hemorrhage occurs in severely injured areas. It is surrounded usually by non-hemorrhagic necrotic tissue [20, 21].

## 1.3 Cardiovascular MRI

Significant advances were necessary to get from the basic principles of NMR to the generation of images of the human body. MRI has revolutionized medical imaging for many organ systems. Due to the motion of the heart, however, the development of cardiac MRI was slower than that of MRI for other organs due to the requirement for faster acquisition techniques. Compared with any other body structures, the ever-pumping heart in the respiratory-tided thorax represents the most difficult organ to image [22]. With advancements in MRI technology, these obstacles have been overcome and cardiac MRI has become a validated tool for imaging the heart.

### 1.3.1 Pulse sequences

Pulse sequences are a pattern of radiofrequency pulses and magnetic gradients that are used to produce an image. There are a variety of different pulse sequences that are used in cardiac imaging. Not intended to be exhaustive, we are listing the most often used techniques for cardiac MRI.

Spin-echo (SE) sequence is one of the oldest pulse sequences used for imaging [23]. Because of the long acquisition time with SE, its faster version, Turbo-spin-echo Sequence (TSE) is used recently. The most frequent application of TSE sequences is the T2-weighted edema imaging in myocardial infarct. High spatial resolution breathhold T1 Turbo-spin-echo imaging with and without fat saturation allows detailed differentiation between myocardium, epicardial fat, trabeculae and myocardial fatty infiltration in Arrythmogenic Right Ventricular Cardiomyopathy (ARVC) [23].

Gradient echo (GE) sequences allow significantly shorter acquisition times to be achieved than with spin-echo sequence. Its variant, Fiesta provides high blood/myocardium contrast, makes it suitable for wall motion analysis and accurate noninvasive determination of different

hemodynamical parameters. Inversion Recovery Fast Gradient echo sequences are used to null the signal from a desired tissue to accentuate surrounding pathology. A common use of this technique is to null the signal from normal myocardium during delayed enhanced (DE) imaging (see later). The nulled normal myocardium will be dark in contrast to the enhanced abnormal myocardium. IR pulses have a special parameter known as inversion time (TI). When attempting to null normal myocardium, one must find the appropriate TI at which the normal myocardium is dark. To determine the appropriate TI for an individual, a TI scout series is obtained where each image in the series has a progressively larger TI.

### 1.3.2 MRI Contrast Agents

#### 1.3.2.1 Overview

High spatial resolution MRI is sometimes performed with the use of intravenous contrast agents to enhance the signal of pathology or to better visualize the blood pool or vessels. Despite the fact that MR images were initially thought to provide enough endogenous contrast, the utilization of exogenous MRI contrast agents (CAs) has increased steadily to reach approximately 40–50% of the examinations currently performed [24]. Most MRI contrast agents are Gadolinium chelates. Gadolinium ion ($Gd^{3+}$) complexes (chelates) with a high thermodynamic and kinetic stability are required for the use of Gadolinium ion in vivo, giving appropriate biodistribution and safety profile [4]. Namely, Gadolinium cannot be used as CA in its $Gd^{3+}$ ionic form, due to its high toxicity and undesirable biodistribution (accumulating in bones, liver or spleen). $Gd^{3+}$, like any other metal ions with one or more unpaired electrons is paramagnetic, and therefore possesses a permanent magnetic moment [25].

The paramagnetic effect of gadolinium causes a shortening of T1 relaxation time, leading areas with gadolinium to be bright on T1-weighted images. The efficiency of MRI contrast agents is

denoted by their R1 relaxivity values, which indicates their ability to decrease T1 relaxation times of the water protons per mM unit concentration of $Gd^{3+}$ ion. The concentration of the contrast agent in a given tissue depends on the ratio between the uptake and the release of the agent. The contrast enhancement is obtained when the concentration of CA in one tissue is higher than the concentration in another one. T1-weighted images give positive image contrast, as the image signal intensity increases at the tissue site where the CA concentrates is dominated by T1 shortening. Contrast agents are used in Cardiac MRI for evaluation of myocardial perfusion, delayed enhanced imaging (myocardial infarctions, infiltrative processes, myocarditis), differentiation of intracardiac masses (neoplasm vs. thrombus) and to opacify blood vessels or left atrium in MR angiography (MRA).

#### 1.3.2.2 Classification of Contrast Agents for MRI

MRI contrast agents represent a heterogeneous class of diagnostic agents. The most common base for classification is their distribution in the body. The distribution of the contrast agent in the tissue is determined by its molecular weight, shape and charges [23].

##### 1.3.2.2.1 Extracellular MRI Contrast Agents

After intravenous injection, extracellular contrast agents quickly and freely distribute to the extracellular space [26]. The terminal half-life for blood elimination is about 1.5 hours for all these compounds when administered to subjects with normal renal function. The steady-state volume of distribution from various pharmacokinetic studies ranges from 210 to 280 mL/kg, consistent with an extracellular distribution. These compounds are eliminated almost exclusively via the kidneys.

Because of their common extracellular distribution, administration of any of these agents yields the same diagnostic information. These contrast agents also allow possible diagnosis of certain pathological conditions with altered distribution space [22]. The altered distribution space at vascular level could be hemangioma and blood-brain barrier breakdown, at interstitial level could be regenerative fibrosis, and at cellular membrane integral level could be tissue necrosis or infarction, eg. myocardial infarct. Lack of real tissue and/or disease specificity of these contrast agents has prompted further research and development of more specific contrast agents.

#### 1.3.2.2.2 Intravascular MRI Contrast Agents

Intravascular or blood-pool type expression refers to a variety of contrast agents that are confined by purpose to the intravascular space and dedicated exclusively to cardiovascular applications. The restriction to the intravascular space can be achieved either by reversible binding of the contrast agent to plasma albumin (e.g. vasovist [27, 28]) or by the large molecular size of the agent which prevents its extravasation through the microvascular wall for some period of time (e.g. vistarem [29, 30]). The major advantages of using intravascular agents include a long plasma half-life, minimal leakage into the interstitial space, high relaxivities (R1), allowing decreased molar dosing.

### 1.3.3 MRI of Myocardial Infarct

#### 1.3.3.1 Viability Assessment with Delayed Enhancement CMR

Differentiation between viable and infarcted tissue and the quantification of their proportion is necessary for clinical decision making. Clearly viable but hibernated myocardium may exhibit functional recovery following revascularization of the involved coronary artery by either percutaneous coronary intervention (PCI) or coronary artery bypass graft (CABG) [31]. Patients

with decisively *nonviable* myocardium, on the other hand, must not be jeopardized needlessly with the high risk procedures of revascularization [32].

The main application of cardiac MRI is the viability assessment following myocardial infarct. A large number of studies have provided considerable information on the value of MRI in myocardial infarction. After injection of an extracellular contrast agent (for example, Gd(DTPA)), its plasma concentration will reach a maximum value and rapidly decrease due to diffusion to the interstitial space and renal washout. Contrast agents diffused to the interstitial space will be resorbed into the capillary bed and undergo renal excretion. However, when the tissue is damaged, for example due myocardial infarction, the resorption rate of contrast agent will be diminished. At 15 to 30 minutes after contrast injection, washout will be complete in normal myocardium in contrast to infarcted. This phenomenon is called "delayed enhancement" (DE) or "late gadolinium enhancement" (LGE) imaging [33].

In the last decade, delayed enhancement inversion recovery gradient echo (IR-GRE) MRI with standard extracellular contrast agents became the most important and accurate imaging tool for assessing either the localization, the transmurality, or the extent, of MIs [34]. DE is also capable of differentiating stunned myocardium from necrotic tissue in the acute phase [35], and hibernated myocardium from scar tissue in the chronic phase, of a MI [31]. Correspondence between location, spatial extent, and 3D shape of the hyperenhanced regions on DE images and the irreversibly injured tissue defined by histomorphometry has been demonstrated [35, 36].

#### 1.3.3.2 Determination of the Age of Myocardial Infarct

A significant number of heart patients suffer a *second* heart attack after their first infarction. Myocardial reinfarction happens in 7-8% of patients with previous MI [37, 38]. According to

recent data [39], the rate of reinfarction is ~ 3% already in the first year in patients with MI treated primarily with balloon angioplasty with or without stenting. Differentiation between acute and older myocardial infarcts is of great importance in clinical decision-making. There are several clinical scenarios where differentiation between acute and older myocardial infarct may be crucial. Differentiation between acute and older MIs, however, represents a challenge for existing imaging modalities [40]. Wall motion abnormalities detected with either Echocardiography, CT, or MRI are not restricted to acute events. In radionuclide imaging, radioactive tracers are not taken up by the non-viable myocardial cells regardless of the age of the MI. Therefore, both recent and long-standing MI appears as a fixed defect. Thus, a fully reliable method is needed which would determine the age of infarct.

A significant shortcoming of the Delayed Enhancement-MRI method is, that standard extracellular contrast agents used with DE-MRI highlight both the acute and the chronic MI. Also, the magnitude of signal intensity enhancement is the same in the territory of a MI in the two stages [35, 41].

We have developed a family of CAs for MRI diagnosis of ischemic heart disease (IHD) [42-45]. Among these, Gd(ABE-DTTA) is optimal for cardiovascular purposes. Gd(ABE-DTTA), which is still under investigation, is the Gadolinium complex of N-(2-butyryloxyethyl)-N'-(2-ethyloxy-ethyl)-N,N'-bis[N",N"-bis(carboxymethyl)acetamido]-1,2-ethanediamine. Recent results show that our method differentiates between acute and older myocardial infarct using myocardial delayed-enhancement magnetic resonance imaging by this new contrast agent.

### 1.3.4 Detection of reversible ischemia with Dobutamine stress MRI in patients with PAD

#### 1.3.4.1 Introduction

The examination of patients with PAD is often not possible or significantly limited with conventional noninvasive cardiac tests because of the followings. Exercise ECG cannot be implemented due to the short intermittent claudication distance [46] of the patient. Patients with PAD often have chronic obstructive pulmonary disease (COPD) as a smoking related disease [47]. Therefore, basic hemodynamic measurements or assessment of wall motion abnormalities with transthoracic rest or stress echocardiography is often not possible or limited [48]. Dypiridamole or adenosine stress testing could be risky in patients with COPD and bronchospasm because of adverse reaction of these stressors [49-51]. To find a diagnostic imaging method for the cardiac assessment for these patients could help to identify those who are at high risk for undesirable cardiac events. Several noninvasive techniques are available for evaluating reversible myocardial ischemia; however, many coronary angiograms yield negative results that may be explained by low diagnostic accuracy of most noninvasive tests. Dobutamine stress MRI (DSMRI) which has grown to a clinically established test in the last two decades is able to identify patients with high risk for cardiac mortality and myocardial infarct [52]. This method based on the above detailed reasons enables the noninvasive assessment of severe coronary artery disease even in patients with PAD. The role of DSMRI, however, is unknown to date in this patient population either from Hungarian or from international scientific literature.

Our recent results show that DSMRI is feasible with low risk for the cardiology assessment of patients with peripheral arterial disease.

# 2 OBJECTIVES AND HYPOTHESES

## 2.1 Overall Goal of the Thesis Project

In the present work, the main goal was to develop a new method that differentiates between acute and older myocardial infarcts, allowing in vivo infarct age determination by delayed-enhancement magnetic resonance imaging using a new contrast agent and to prove that Dobutamine stress MRI is safe and feasible method for the noninvasive cardiac assessment of patients with PAD, yielding identification those who are at high risk for undesirable cardiovascular events.

## 2.2 The first series of the investigation

**In the first series** of our investigations we aim to examine the ability of our method to differentiate between acute and 4 week old infarcts in vivo in a subject having both type of myocardial infarct. For that specific aim a canine, closed chest, reperfused, double infarct model will be used. Two myocardial infarcts will be generated in the animals by occluding the Left Anterior Descending (LAD) coronary artery with an angioplasty balloon for 180 min, and four weeks later occluding the Left Circumflex (LCx) coronary artery. Using this model, the age of the infarct will be determined by its location. Two different contrast agents will be tested. The first agent will be a standard extracellular contrast agent, Gadolinium diethlynetriamine penta-acetic acid, Gd(DTPA). This agent is the most frequently used agent for delayed enhancement MRI. The second agent will be Gd(ABE-DTTA), the new, low molecular weight contrast agent. Inversion-recovery gradient-echo (IR-GRE) images will be obtained on day 3 and day 4 after second myocardial infarct, using Gd(DTPA) and Gd(ABE-DTTA), respectively. Triphenyltetrazolium chloride (TTC) histomorphometry will validate the existence and location

of infarcts. Hematoxylin-eosin and Masson's trichrome staining will provide histologic evaluation of infarcts. The signal intensity enhancement will be determined in the two different age of myocardial infarct.

Our assumption is that the two contrast agent will exhibit different behavior during Delayed Enhancement MRI. We anticipate that Gd(ABE-DTTA) or Gd(DTPA) will highlight the acute infarct, whereas the four-week old infarct will be visualized only by Gd(DTPA), but not by Gd(ABE-DTTA).

We hypothesize the followings:

1. With Gd(ABE-DTTA), the mean signal intensity enhancement (SIE) will be significantly higher in the acute infarct than in the four-week old infarct.
2. With Gd(ABE-DTTA), the mean signal intensity enhancement in the four-week old infarct will not differ significantly from that of in healthy myocardium.
3. Gd(DTPA) will produce similar signal intensity enhancements in acute and four-week old infarcts, i.e. the two values will not differ statistically significant.
4. The signal intensity enhancement in acute or 4 week old myocardial infarct induced by Gd(DTPA) will not be statistically different from Gd(ABE-DTTA)-induced SIE in acute infarct.

The four hypotheses together involves that Gd(ABE-DTTA) differentiates between acute and 4 week-old infarcts, and induces the same SIE in acute infarcts as Gd(DTPA) does.

### 2.3 The second series of the investigation

**In the second series** of our investigations we aim to determine the affinity of Gd(ABE-DTTA) during the subacute phase of scar healing, and to compare it to the affinity during the late

subacute phase already studied in the first series of our investigations. To implement that comparison, a different MI model and experimental design will be used. For that specific aim a canine, closed chest, reperfused, single MI model will be used in a longitudinal study. In this series of our investigations a single MI will be generated by occluding for 180 min the Left Anterior Descending (LAD) coronary artery with an angioplasty balloon. This single infarct will be followed up by the new low molecular weight contrast agent, Gd(ABE-DTTA)-enhanced DE-MRI. DE-MRI images will be obtained on days 4, 14, and 28 after MI with Gd(ABE-DTTA). In addition, control visualization of the infarct by a standard extracellular contrast agent, Gd(DTPA) (it is also used in the first series of the investigation) will be carried out on day 27, to ascertain that the infarct will be still in place even when the acute-infarct specific agent did not highlight it. T2- weighted TSE images will be acquired on day 3, 13 and 27. Triphenyltetrazolium chloride (TTC) histomorphometry will test postmortem (day 28) the existence of infarct.

Our assumption is that the new contrast agent will exhibit different behavior during Delayed Enhancement MRI in the different ages of the infarct scar development. We anticipate that infarct affinity of Gd(ABE-DTTA) disappears already in the subacute phase of scar healing, i.e. Gd(ABE-DTTA) will highlight the infarct on day 4, but not on day 14 or on day 28 following MI. We also anticipate that the conventional T2-weigted edema imaging highlights the infarcts and the segments supplied by the infarct-related artery ("area at risk") similarly in the acute, subacute and late subacute phase, i.e. T2w imaging is not able to distinguish among these different phases of the myocardial infarct healing during the time window the study uses.

We hypothesize the followings:

1. On day 4, the mean signal intensity (SI) of infarcted myocardium in the presence of Gd(ABE-DTTA) will significantly differ from that of healthy myocardium, but it will not on day 14, nor on day 28.
2. The mean signal intensity enhancement (SIE) induced by Gd(ABE-DTTA) on day 4 will be significantly different from mean SIE on day 14, and from mean SIE on day 28 following MI.
3. The mean SIE values induced by Gd(ABE-DTTA) on day 14 and on day 28 will not differ significantly between them.
4. Gd(DTPA) will highlight the infarct on day 27.
5. The mean SIE on day 3, 13, or 27 will not vary significantly (P=NS) on the T2-TSE images.

The five hypotheses together involve that Gd(ABE-DTTA) differentiates similarly between acute and 2-week-old MI as it does between acute and 4-week old MI, while conventionally used T2-weighted edema imaging does not have similar properties.

### 2.4 The third series of the investigation

**In the third series** of our investigations we aim to prove that Dobutamine stress MRI is a safe and feasible method for the noninvasive cardiac assessment of patients with PAD. For that specific aim 21 patients with peripheral artery disease will be studied prospectively with dobutamine stress cardiovascular MRI. To attain the 0.85 × (220 – age) target heart rate, the dose of Dobutamine will be elevated up to 40 μg/kg/min and supplemented with 0.25 mg/min Atropine up to 1 mg if require. The stress will have been terminated before target heart rate will

be reached if inducible wall-motion abnormalities appear or angina occurs. Following stress, Gd(DTPA) will be given and late enhancement (LE) MRI will be implemented. MRI images will be analysed independently by two senior cardiologists experienced in cardiac imaging and having European accreditation for CMR. The readers will be blinded to the clinical data of the patients. Standardized scoring system (1=normokinetic 2=hypokinetic 3= akinetic 4= dyskinetic) and the 17-segment model of the American Heart Association will be applied. The interobserver agreement for the assessment of wall motion abnormalities will be calculated. Image quality of different anatomical localizations will be graded on a 4-point scale based on the visibility of the endocardial border at rest and during stress. Image quality between different anatomical localizations will be analyzed. Difference of image quality of four anatomical regions (anterior, lateral, inferior, and septal) at rest or during stress will be studied. Symptoms, side effects, and adverse events will be recorded. The rate of inducible wall motion abnormalities will be determined.

Our assumption is that different aspects of feasibility and safety will be acceptable in this group of patients.

We hypothesize the followings:

1. The interobserver agreement for the assessment of wall motion abnormalities will be at least good.
2. Median [interquartile range] image quality score for all anatomical localizations will be at least good (3 [3-3]) on the 4-point scale either at rest or during stress.
3. The median image quality will not be change significantly between different anatomical localizations.

4. There will not be statistical difference between image quality of four anatomical regions (anterior, lateral, inferior, and septal) at rest or during stress.
5. The protocol of the study will be completed by a significant number of the patients.
6. The target heart rate will be attained in a high proportion of the studies.
7. The side effects could be regarded to be acceptable, and serious adverse events will be rare.

The seven hypotheses together involve that Dobutamine stress MRI is a safe and feasible method for the noninvasive cardiac assessment of patients with PAD.

# 3 DIFFERENTIATION OF ACUTE AND FOUR-WEEK OLD MYOCARDIAL INFARCT WITH GD(ABE-DTTA)-ENHANCED CMR

## 3.1 Introduction

Reinfarction occurs in 7-8% of cardiac patients with previous MI [37, 38]. In a recent meta-analysis [39], with 6921 patients with MI treated primarily with balloon angioplasty with or without stenting, the rate of reinfarction was ~ 3% in the first year. Differentiation between acute and older MIs is of great importance in clinical decision-making. Wall motion abnormalities detected with echocardiography, computed tomography (CT), or cardiovascular magnetic resonance (CMR) are not restricted to acute events. Also, regardless of age of MI, radioactive tracers are not taken up by non-viable myocardial cells imaging, and therefore both recent and long-standing MI appears as a fixed defect. Not even late enhancement (LE) CMR with standard extracellular contrast agents (CA) like Gadolinium-DTPA (Gadolinium-Diethylenetriaminepentaacetic acid) differentiates by age of infarct [53, 54].

We have developed a family of CAs for CMR diagnosis of ischemic heart disease (IHD) [42-45]. Among these, Gd(ABE-DTTA) is optimal for cardiovascular purposes. Gd(ABE-DTTA), which is still under investigation, is the Gadolinium complex of N-(2-butyryloxyethyl)-N'-(2-ethyloxy-ethyl)-N,N'-bis[N",N"-bis(carboxymethyl)acetamido]-1,2-ethanediamine. This low molecular weight (764 Dalton) agent's clearance from the blood has a kinetics similar to that of blood pool contrast agents, although it also displays partly extracellular characteristics [55]. It demonstrates high affinity for acute MI [55]. The acutely infarcted tissue takes up Gd(ABE-DTTA) within a longer period of time than it does purely extracellular contrast agents. The maximum concentration of the agent in the acutely infarcted tissue shows up at 48 hr, although it is not significantly different from that which is already achieved at 24 hr, and the contrast remains

detectable in the infarct up to 12 days [55]. The agent causes no deleterious physiological effects, and a previous study has demonstrated the short- and long term safety of its usage [56].

Gd(ABE-DTTA) has been successfully used for continuous detection of myocardial ischemia during 30 min of left anterior descending coronary artery (LAD) occlusion [57, 58]. The suitability of Gd(ABE-DTTA) for accurate quantification of acute MI has also been demonstrated [59, 60].

In this study we have shown that Gd(ABE-DTTA) induces a LE effect in acute, but not in late subacute MI.

## 3.2 Methods

### 3.2.1 Gd(ABE-DTTA) sample preparation

Gd(ABE-DTTA) was synthesized, and samples were prepared, as described by Saab et al. [44]. To guarantee consistent quality of agent before administration the in vitro relaxivity was measured for every sample [44]. Each animal received Gd(ABE-DTTA) at the dose of 0.05 mmol/kg, the in vitro relaxation enhancement of which was equivalent to that of Gd-DTPA at its conventional dose (0.2 mmol/kg) used for LE-CMR.

### 3.2.2 Study design

Animals were studied with a closed-chest, reperfused, double MI protocol described below. The smallest number of animals (n=6) that still achieved statistical significance was used. MIs were generated in the LAD coronary artery territory and four weeks later in that of the left circumflex coronary artery (LCx) (Fig. 1.). To avoid a confounding, simultaneous action of the two contrast agents, two separate CMR sessions were carried out 3 and 4 days after the generation of the second MI, separately using Gd(DTPA) and Gd(ABE-DTTA) in these two sessions, respectively.

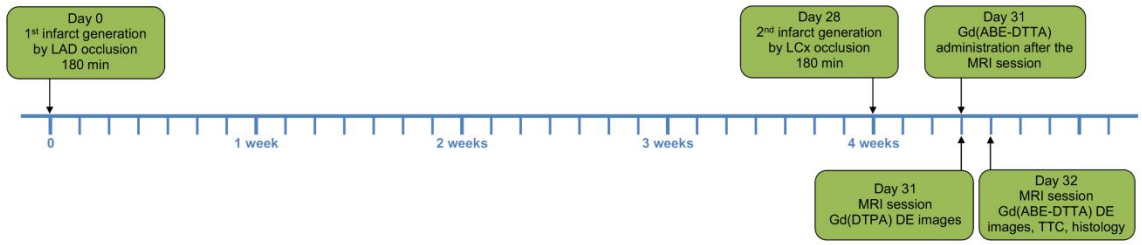


**Fig. 1 - Timeline of the Study Protocol – Double Infarct Model**

Day 0 - MI generation in LAD-supply area. Day 28 - another MI generation in LCx- supply area. Day 31 (3 days after the 2nd MI) - CMR session: obtaining LE images with Gd(DTPA), thereafter administering of Gd(ABE-DTTA). Day 32 (4 days after the 2nd MI) - CMR session: obtaining LE images with Gd(ABE-DTTA), followed by TTC, and histology

### 3.2.3 Surgical procedure

Animal protocol was approved by the University of Alabama at Birmingham IACUC in full compliance with the 'Guidelines for the Care and use for Laboratory Animals' (NIH). Six male hounds (18-20 kg) were used. Twelve hours prior to procedure food was taken away and 325 mg Aspirin given. Dogs were anesthetized with a Ketamine (5.0mg/kg) and Diazepam (0.5mg/kg) mixture, intubated, and connected to a Hallowell EMC Model 2000 respirator (Pittsfield, MA, USA) operated with a tidal volume of 400 ml at a rate of 16 BPM. Anesthesia was maintained by continuous Isoflurane (2.5-3 volume %), and repeated Fentanyl (50-100ug I.V. every 30 minutes), administration. Heart rate and blood oxygen saturation were monitored using a pulse-oxymeter placed on the animal's tongue. ECG electrodes were placed on the chest to record electrophysiological signs of myocardial ischemia and arrhythmias. The left femoral artery was separated surgically and an arterial sheath (6-8 French) was inserted. An I.V. line was placed to administer infusion and drugs. Heparin (100 IU/kg) was given intravenously to maintain the activated clotting time (ACT) above 300 seconds. A properly sized 2-3 mm angioplasty balloon was introduced under fluoroscopic guidance into the LAD (1st infarct) or the LCx (2nd infarct)

and inflated for 180 minutes to create MI. Thereafter, the balloon was deflated to restore coronary circulation. Coronary angiography confirmed the reperfusion after balloon deflation.

On days 3 and 4 after the second infarction, animals were re-anesthetized as described above and CMR studies performed. Animals were then sacrificed, hearts excised and embedded in agar. The agar block was cut perpendicular to the long axis with a commercial meat slicer into 5 mm sections starting from the apex. 2,3,5-triphenyltetrazolium chloride (TTC) was dissolved in physiological saline to obtain 2% TTC solution. Slices were immersed in it at 37◦C for 15 min and then rinsed with physiological saline. All TTC-stained slices were photographed with a high resolution digital camera. TTC-stained slices were used to validate the existence and location of infarcts.

### 3.2.4 Magnetic Resonance Imaging

A 1.5T GE Signa-Horizon CV/i scanner (Milwaukee, WI, USA) was used. A cardiac phased-array coil and ECG gating were employed. Breath-hold was performed at end-expiration. A $180^{o}$-prepared, segmented, inversion-recovery fast gradient-echo pulse was used with: Field of View (FOV) 30 cm, Echo Time (TE) 3.32 ms, Repetition Time (TR) two cardiac cycles (1100-1600 ms), slice thickness 10 mm. The Inversion Time (TI) was optimized to null the signal of normal myocardium. Conventional cardiac angulation planes were set and short axis slices covering the entire left ventricle (LV) obtained (six slices per heart).

In the first CMR session, a 0.2 mmol/kg Gd(DTPA) (Magnevist, Schering, Kenilworth, NJ) bolus was administered intravenously. LE images were acquired 15-20 min thereafter. Gd(ABE-DTTA) was given intravenously at the end of the first CMR session. In the second CMR session, 24h after Gd(ABE-DTTA) administration, LE images were similarly obtained.

### 3.2.5 Histology

Post mortem tissue samples from the infarct and the peri-infarct regions were examined by histopathology. The samples were fixed in 10% formalin, embedded in paraffin, and sectioned at 5 m thickness. Hematoxylin-eosin and Masson's trichrome staining was performed.

### 3.2.6 Image analysis

The existence of both acute and four-week old infarcts was validated and their anatomical localization determined by analyzing the TTC images. CMR Dicom images were imported as image sequences with the use of ImageJ (Wayne Rasband, NIH). The endo- and epicardial contours of the LV muscle were traced manually and this circumscribed area was further analyzed. Based on the apicobasal localization and anatomical landmarks (LV and papillary muscle shape, and the position of the anterior and posterior interventricular grooves), CMR images acquired in the presence of the two different contrast agents, as well as the TTC slices, were matched. All CMR slices that contained a MI according to the corresponding TTC slices were categorized into four groups by anatomical localization of the infarct to either the four-week old or to the acute category, and by the contrast agent given.

To separate the acute and the four-week old infarcts for the analysis, the images of slices containing both types of MI were partitioned into two images, each reflecting one half of the tomographic slice. The partition was done, with ImageJ, along a straight line starting at the posterior interventricular groove (0° on the LV circumference), through the center point of the LV slice, ending at the 180° point on the LV circumference in the anterolateral region. Thus four groups of images were obtained for analysis: $Gd(DTPA)_{acute}$, $Gd(DTPA)_{4week}$, $Gd(ABE\text{-}DTTA)_{acute}$, $Gd(ABE\text{-}DTTA)_{4week}$, to which two control groups, ($Gd(DTPA)_{normal}$, Gd(ABE-

DTTA)$_{normal}$), i.e. normal myocardium with each of the two agents, have been added, bringing the number of data groups for analysis to six.

To avoid observer bias, instead of manual contouring of the infarct and the healthy myocardial regions, a pixel-by-pixel analysis was performed. The pixel-by-pixel SI histogram of every CMR image, segmented in the above manner, was generated with ImageJ and these histograms were used for further analysis. First, the mean SI ±SD of healthy myocardium was determined by exporting the histograms to Origin 7.0 (OriginLab Corporation, Massachusetts, USA), and employing Gaussian curve fitting on each using the Levenberg-Marquardt algorithm [61]. In agreement with a previous publication [62], pixels with SI above the mean + 6 SD of the normal myocardium were regarded as enhanced pixels, i.e. pixels of the infarct. The mean SI of these enhanced pixels was calculated from this set of pixels in each image. If no pixels above the threshold were found, the mean signal intensity of the infarct was concluded to be equal to that of healthy myocardium. The mean SIE in each pixel was computed by [63]:

$SIE=100 \times (SI_i - SI_n) / (SI_n)$,

where $SI_i$ and $SI_n$ are the mean signal intensity in infarct and normal myocardium, respectively.

### 3.2.7 Statistical analysis

Results are reported as mean ± SD. Statistical analysis was carried out by SigmaStat (version 2.03; SPSS Inc, Chicago, IL, USA). Two-way repeated measures analysis of variance was used to compare the SIE values among the six experimental groups. Normal distribution and equality of variances were tested. Although the test of normality failed, due to the equality of variances, the equality of group sizes, and the high power of the performed test (0.985 with $\alpha=0.05$), the assumption of the F test in the two-way ANOVA with repeated measures was not violated [64]. Since an overall significance ($P<0.05$) was established for rejecting the null hypothesis that the

six groups are not different, pairwise differences between the groups were assessed by using the Holm-Sidak method of adjustment for multiple comparisons.

### 3.3 Results

Both the acute (LCx) and four-week old (LAD) infarcts were visible in Gd(DTPA)-enhanced LE images of all six dogs. The existence and localization of recent and four-week old infarct were confirmed by TTC. Histologic evaluation confirmed acute infarcts with coagulation necrosis, inflammation (mostly mononuclear), and multiple foci of calcification in the 4 days old infarct areas (Fig. 2).

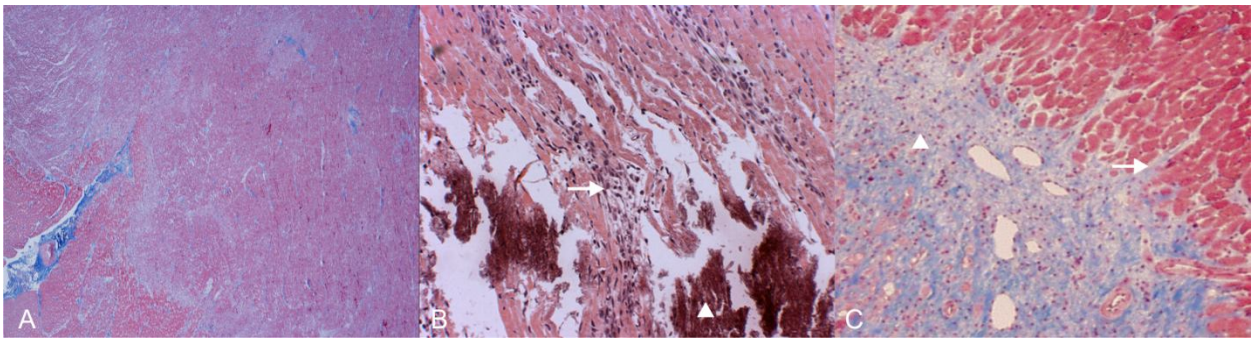


**Fig. 2 – Double Infarct Histology**

Histologic section of a dog LV 32 days following the first (LAD), and 4 days after second (LCx), MI. (A) Acute (LCx) MI with coagulation necrosis, inflammation and multiple foci of calcification (40x, Masson's trichrome). (B) Same area at higher magnification. Dying myocardial fibers (white arrow) associated with inflammatory cells, Calcium precipitates (white arrowhead) (100x). (C) Late subacute (LAD) MI in the same heart with granulation tissue (white arrowhead) and early collagen deposition, interdigitating (white arrow) with viable myofibers (40x, Masson's trichrome).

Healing with granulation tissue and early collagen deposition, and small areas of interstitial fibrosis adjacent to the late subacute infarct were seen in the four-week old infarct areas. Gd(ABE-DTTA) did not induce SIE in the subacute (LAD) infarcts, while the acute (LCx) infarcts were clearly visible on LE images of all six animals in the presence of this CA (see examples in Fig. 3, 4, and 5).

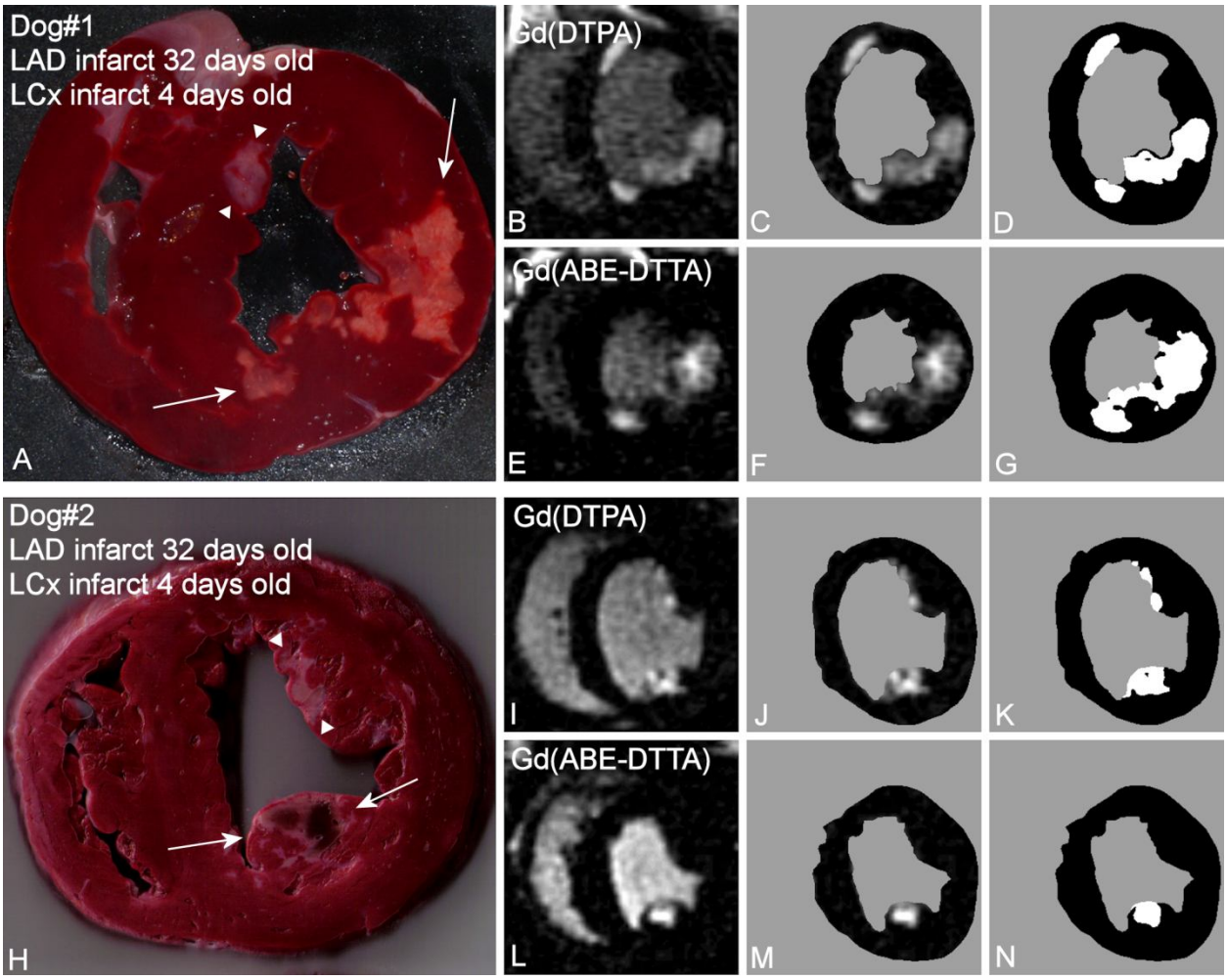


**Fig. 3 - Differentiation between Acute vs. Subacute Myocardial Infarctions**

A: TTC stained photograph of a canine (Dog#1) transversal LV slice 32 days following the first (LAD) and 4 days after second (LCx) infarct. White arrows point to the acute infarct located in the posterior and postero-lateral segments (LCx-supply area). Subacute infarct (white arrowheads) is seen on the border of the anteroseptal and anterior segment (LAD-supply area). B: Corresponding LE CMR image taken in the presence of Gd(DTPA). This CA does not differentiate between the acute and the subacute infarcts. C: Same as B, after the endo- and epicardial contours of the LV muscle had been traced manually D: Image in C thresholded at normal+6SD intensity. E: Same CMR image as in B, taken in the presence of Gd(ABE-DTTA) one day following B. Only the posterior and postero-lateral segments, i.e. the acute infarct, show LE. The subacute infarct is not highlighted by this agent, thereby differentiating between acute and subacute infarcts. F: Same as E, after the endo- and epicardial contours of the LV muscle had been traced manually. G: Image F thresholded at normal+6SD intensity.
H: TTC photograph of *another* canine (Dog#2) LV slice 32 days following first (LAD) and 4 days after second (LCx) infarct. White arrows point to the acute (hemorrhagic) infarct in the posteromedial papillary muscle (LCx-supply area). Subacute infarct (white arrowheads) is seen predominantly in the anterolateral papillary muscle (LAD-supply area). I: Corresponding LE image with Gd(DTPA). J: Same as I, after the contours of the LV muscle had been traced K: Image J thresholded at normal+6SD L: Same CMR image as in I, taken in the presence of Gd(ABE-DTTA) one day following I. Only the acute infarct shows LE. The subacute infarct is not highlighted by this agent.

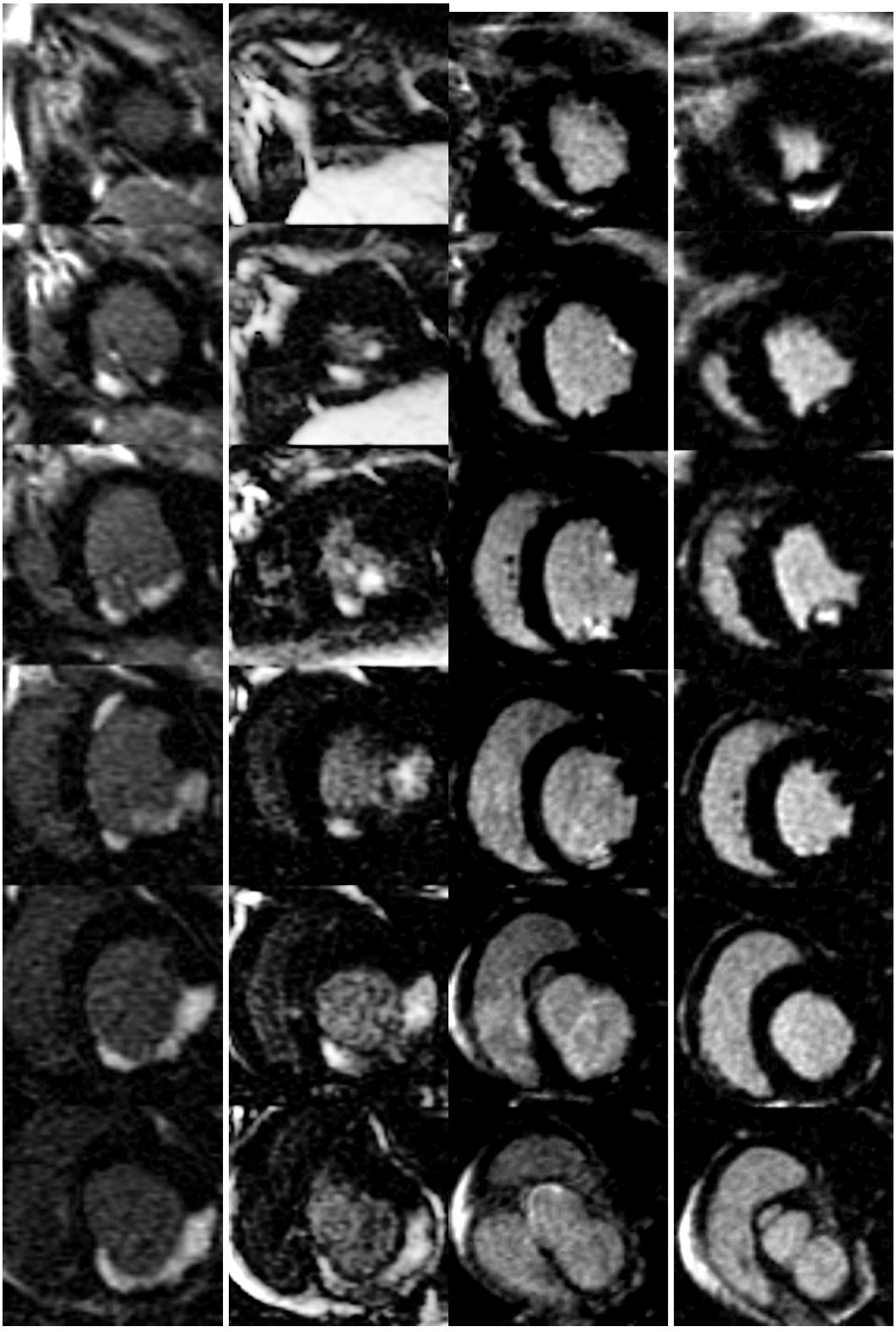

**Fig. 4 and 5–Short Axis LE CMR Image Set –Dog#1 and Dog#2**

All base-apex slices of dog#1 and dog#2 (see also Fig. 3). Left column – LE images with Gd(DTPA). Right column - LE images with Gd(ABE-DTTA).

Mean ±SD SIE values are shown in Table 1 and Fig. 6. With Gd(ABE-DTTA), the mean SIE in the areas with acute infarct was 366 ± 167 %, whereas in areas of four-week old infarcts it was only 24 ± 59 %. The difference is statistically significant (P<0.05). The mean SIE in four-week old infarct areas with Gd(ABE-DTTA) did not differ significantly from SIE of healthy myocardium (P=NS). In contradistinction, Gd(DTPA) produced similar mean SIEs in acute (430 ± 124 %) and four-week old infarcts (400 ± 124 %, P=NS). Furthermore, the mean SIE values of neither acute nor four-week old infarcts enhanced with Gd(DTPA) were statistically different from mean SIE of acute infarct areas enhanced with Gd(ABE-DTTA). These data show that Gd(ABE-DTTA) differentiates between acute and 4 week-old infarcts, and induces approximately the same SIE in acute infarcts as Gd(DTPA) does.

**Table 1 - Contrast Induced by the Two Agents in Acute versus Subacute Infarcts**

| | Gd(ABE-DTTA) | | Gd(DTPA) | |
|---|---|---|---|---|
| Parameter | Acute infarct | Subacute infarct | Acute infarct | Subacute infarct |
| SIE (%)* | 366±166 | 24±59 | 431±124 | 400±124 |
| P value† vs. normal myocardium | P<0.05 | NS | P<0.05 | P<0.05 |
| P value vs. Gd(ABE-DTTA)$_{subacute}$ | P<0.05 | | P<0.05 | P<0.05 |
| P value vs. Gd(ABE-DTTA)$_{acute}$ | | | NS | NS |
| P value vs. Gd(DTPA)$_{acute}$ | | | | NS |

*Mean ± SD (n=6) signal intensity enhancement (in percent values) by Gd(ABE-DTTA) and Gd(DTPA) in the territory of acute and subacute occlusions

†P values pertain to pairwise comparisons by the Holm-Sidak method of the different subgroups

### 3.4 Discussion

Gd(ABE-DTTA) was capable of differentiating between acute and four-week old infarcts as no LE effect was seen in the latter while one is clearly observable in the former. Acute MIs can be seen on the LE-CMR images enhanced with either Gd(DTPA) or Gd(ABE-DTTA). Older MIs are visible only by Gd(DTPA). Our general observations show in dogs that the agent's affinity to infarcted myocardial tissue disappears between days 10 and 14 following acute myocardial infarction. The question of the detailed kinetics of effect disappearance is currently under investigation.

#### 3.4.1 Magnetic resonance imaging for differentiation between new and longstanding MI

Saeed et al. [65] have recently published similar observations with an intravascular, high molecular weight contrast agent, P792, Vistarem (Guerbet Group, Paris, France). They studied one infarct at two different time-points in a single MI model. The intravascular agent produced a LE in the acute, 3 day old infarct but not in the later, chronic phase, at 8 weeks, after infarction. The authors have also proven the superiority of their method over the T2-weighted (T2w) CMR technique (also see below) for the distinction between acute and chronic myocardial infarct.

Other methods for the differentiation between new and longstanding MIs have also been published. In a recent publication Hillenbrand et al. [66] reported a method with the combination of Gd(DTPA)-enhanced $^{1}H$ MR and $^{23}Na$ MR. Due to granulation tissue infiltrates and collagen deposition, the $^{23}Na$ MR signal intensity in the MI area showed a significant decrease during infarct healing. Another approach by Abdel-Aty et al. [40] combined Gd(DTPA)-induced LE with T2-weighted (T2w) CMR. The distinction was based on an elevated T2w signal intensity due to edema which is located selectively in the newly infarcted tissue [40]. The specificity of this method could be limited by the fact, however, that sometimes, especially in the case of

ongoing residual ischemia, sustained postinfarction edema can be detected for up to one year after MI [67]. Kim et al. [68] used contrast enhanced steady state free precession (SSFP) CMR for the distinction between recent and chronic MIs. The mean signal intensity of acute infarct areas was elevated during SSFP CMR, two minutes after Gd(DTPA) administration. Chronic infarct regions, however, showed signal intensities similar to that of normal myocardium. The exact mechanism of the LE phenomenon is not known to date even for standard extracellular agents. Increased volume of distribution, due to sarcolemmal membrane rupture in acute infarct, and low grade of cellularity with expanded interstitial collagen matrix of chronic scar tissue, have been suggested as potential mechanisms for such agents [35, 36, 53, 54, 69].

### 3.4.2 Histological basis of the CMR observation

The evolution of MI is a complex pathohistological process [70]. Several hypotheses can be brought up to explain the selective accumulation of Gd(ABE-DTTA) into acute MIs. The first is linked to the partial intravascular nature of Gd(ABE-DTTA) [55]. Microvascular damage in an acute infarct [70] could lead to increased microvascular permeability towards CAs with intravascular behavior [71, 72], while the remodeled microvessels in healing infarcts [65, 73] would reduce such permeability. Having partial intravascular characteristics [55], the above mentioned process could increase the wash-in constant of Gd(ABE-DTTA) in acute infarcts, and decrease it in four-week old infarcts. A second hypothesis may be attributable to a possible necrosis-avidity of Gd(ABE-DTTA). There may be binding sites for the CA among the different elements of acute necrotic tissue such as subcellular compartments (ruptured membrane, cytosol, mitochondria), calcium precipitates [70, 74], or ingredients of acute inflammatory reactions, persisting selectively in acutely infarcted tissue. Thus the progressive, persistent [55] accumulation in acutely infarcted tissue of Gd(ABE-DTTA) may be partly due to its partial

lipophilic nature [44], whereby lipids derived from the above mentioned cellular components may trap this CA.

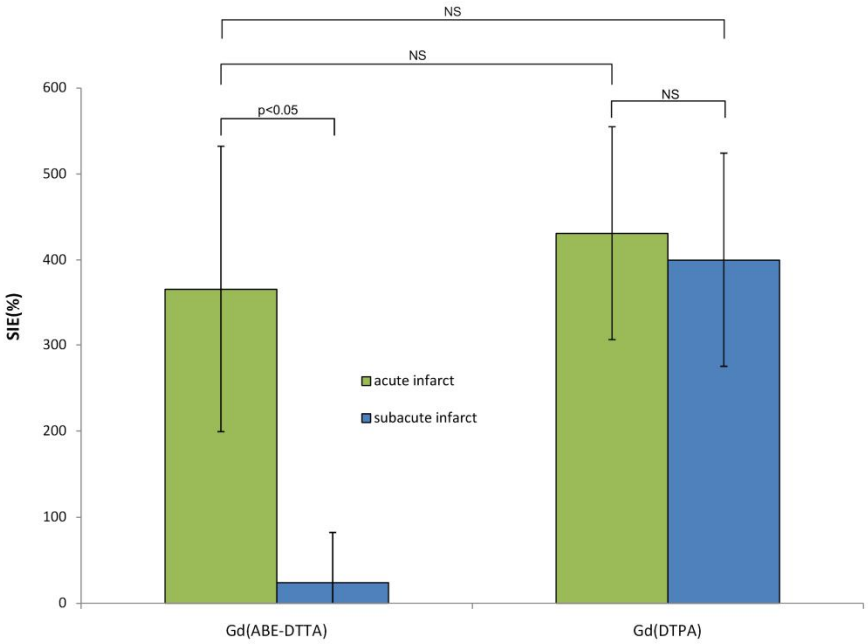


**Fig. 6 - Comparison of SIE Values.**

Mean (n=6) Signal Intensity Enhancement (%) induced by Gd(ABE-DTTA) or Gd(DTPA) in areas of acute (green bars) and subacute infarcts (blue bars).

### 3.4.3 Study limitations

Our study has some limitations. The LE images with the two different CAs were performed on two consecutive days. Thus, small differences in selection of the planes of the short-axis images between the two CMR sessions cannot be completely excluded. These differences, however, would not impair the outcome of our studies.

On day 31, Gd(ABE-DTTA) was administered at the end of the first CMR session. It brings up the possibility, as Gd(DTPA) (in spite of its short half life time) might not have been fully cleared from the body yet, that the two contrast agents could potentially interact with each other. There is no chemical basis, however, for the assumption of interaction, and that it could have influenced the late enhancement phenomenon in the second CMR session, i.e. 24 hours later. Publications [55, 59] already demonstrated the ability of Gd(ABE-DTTA) to detect acute infarcts. These publications used a protocol where Gd(ABE-DTTA) was administered alone.

Gd(ABE-DTTA) needs to be administered 24 hours before CMR imaging, and this introduces an inconvenience in a clinical setting. It may not be convenient (the cardiology ward and radiology are not necessarily close), nor practical for answering the urgent clinical question in a timely fashion. This mode of contrast agent administration, however, is not unknown in the practice of nuclear cardiology. For example, there is a protocol for the assessing of myocardial viability with rest redistribution $^{201}$Thallium SPECT (Single Photon Emission Computed Tomography), where repeated delayed imaging is employed 3-4 h or 24 h following the administration of the radiotracer [75].

The slow clearance of Gd(ABE-DTTA) from the body suggests that the time available for undesired physiological effects, such as dissociation of Gd from the chelate, may be considerably longer than is the case for agents currently approved for human use. It is noteworthy, however, that Gd(ABE-DTTA)'s short- and long term physiological safety has been reported [56].

### 3.5 Conclusions

In summary, we have shown that LE-CMR with separate administrations of Gd(DTPA) and Gd(ABE-DTTA) differentiates between acute and four-week old MIs in a reperfused, double infarct, canine model.

# 4 Acute infarct selective MRI contrast agent

## 4.1 Introduction

Differentiation between acute and older MIs is of great importance in clinical decision-making. There are several clinical scenarios where differentiation between acute and older myocardial infarct may be crucial, such as exclusion of myocardial reinfarction in the presence of an old infarct, or localization of the "culprit" vessel in patients with multi-vessel CAD in acute Non-ST-segment-elevation-MI (NSTEMI) in the presence of an old MI.

In the last decade, delayed enhancement (DE) inversion recovery gradient echo (IR-GRE) MRI with standard extracellular contrast agents became the most important and accurate imaging tool for assessing either the localization, the transmurality, or the extent, of MIs [34]. DE is also capable of differentiating stunned myocardium from necrotic tissue in the acute phase [35], and hibernated myocardium from scar tissue in the chronic phase, of a MI [31]. A significant shortcoming of this method is, however, that standard extracellular contrast agents used with DE-MRI highlight both acute and chronic MI. Also, the magnitude of signal intensity enhancement in the territory of MI in the two stages is similar [35, 41].

We have shown [76, 77] that a low molecular weight MRI contrast agent developed in our laboratory, Gd(ABE-DTTA), induces a DE effect in acute (four-day old), but not in late subacute (four-week old), MI in a canine, *double* infarct model. The infarct affinity of Gd(ABE-DTTA), however, is not known between days 4 and 28 following MI. The purpose of the current study has been the determination of this affinity in the subacute phase of scar healing, and to compare it to the already known affinity during the *late* subacute phase. For the purpose of this comparison, a different MI model and experimental design were applied compared to those previously used [76, 77]. In the present study a *single* myocardial infarct was generated and

followed longitudinally, and determination of the contrast agent's affinity was extended to day 14. This design allowed the comparison of the SIE produced by Gd(ABE-DTTA) on day 4 to those on day 14 as well as on day 28.

Gd(ABE-DTTA) is in investigational phase, and has no deleterious physiological effects [78]. Its clearance from the blood has a kinetics similar to that of blood pool contrast agents, although it also displays partly extracellular characteristics [55]. It demonstrates high affinity for acute MI [55], with slow, distinctive tissue-persistent kinetics. Gd(ABE-DTTA) is taken up into, and is washed out from the acutely infarcted tissue slowly, in contradistinction from the kinetics of standard extracellular agents' uptake and wash-out. This CA attains its maximum concentration in the acutely infarcted tissue around 48 hr after administration, but a useful contrast is already achieved at 24 hr. The contrast remains detectable in the infarct for a few days [55]. Gd(ABE-DTTA) quantifies the extent of acute MI accurately [59, 60].

We hypothesized that Gd(ABE-DTTA) differentiates similarly between acute and 2-week-old MI as it does between acute and 4-week old MI, ie. the infarct affinity of Gd(ABE-DTTA) vanishes already in the subacute phase of scar healing.

## 4.2 Methods

### 4.2.1 Gd(ABE-DTTA) sample preparation and administration

Gd(ABE-DTTA) was synthesized, and samples were prepared, as described by Saab et al. [44]. The in vitro relaxivity was measured for every sample [44] to guarantee consistent quality of agent sample before administration. Gd(ABE-DTTA) was administered at the dose of 0.05 mmol/kg 24 h before every Gd(ABE-DTTA)-enhanced DE-MRI session. This dose was four-

fold lower than the typical dose (0.2 mmol/kg) at which Gd-DTPA had been used for DE-MRI, yet induced an in vitro relaxation enhancement equivalent to that of the higher dose Gd-DTPA.

### 4.2.2 Study design

Dogs (n=7) were studied in a longitudinal, closed-chest, reperfused, single MI model, as follows. MI was generated by occluding for 180 min the LAD coronary artery with an angioplasty balloon. Inversion-recovery fast gradient echo (IR-FGE) MRI images were obtained on days 4, 14, and 28 after MI, and delayed enhancement was generated with Gd(ABE-DTTA). On days 13 and 27 post MI, the same MRI IR-FGE image sequence was used without contrast agent, to demonstrate that the previously administered tissue-persistent CA, Gd(ABE-DTTA), totally cleared from the myocardial infarct as judged by comparison to precontrast images. In addition, control visualization of the infarct was carried out on day 27 with Gd(DTPA) (standard extracellular contrast agent), to ascertain that the infarct was still in place despite the fact that the acute-infarct specific agent did not highlight it. To avoid a potential interaction of the two CAs, Gd(ABE-DTTA) was administered on day 27 only upon the complete clearing of Gd(DTPA). T2-weighted Turbo Spin Echo (T2-TSE) images were acquired on day 3, 13 and 27 before contrast agent administration. Outline of the experimental design is shown in Fig. 7.

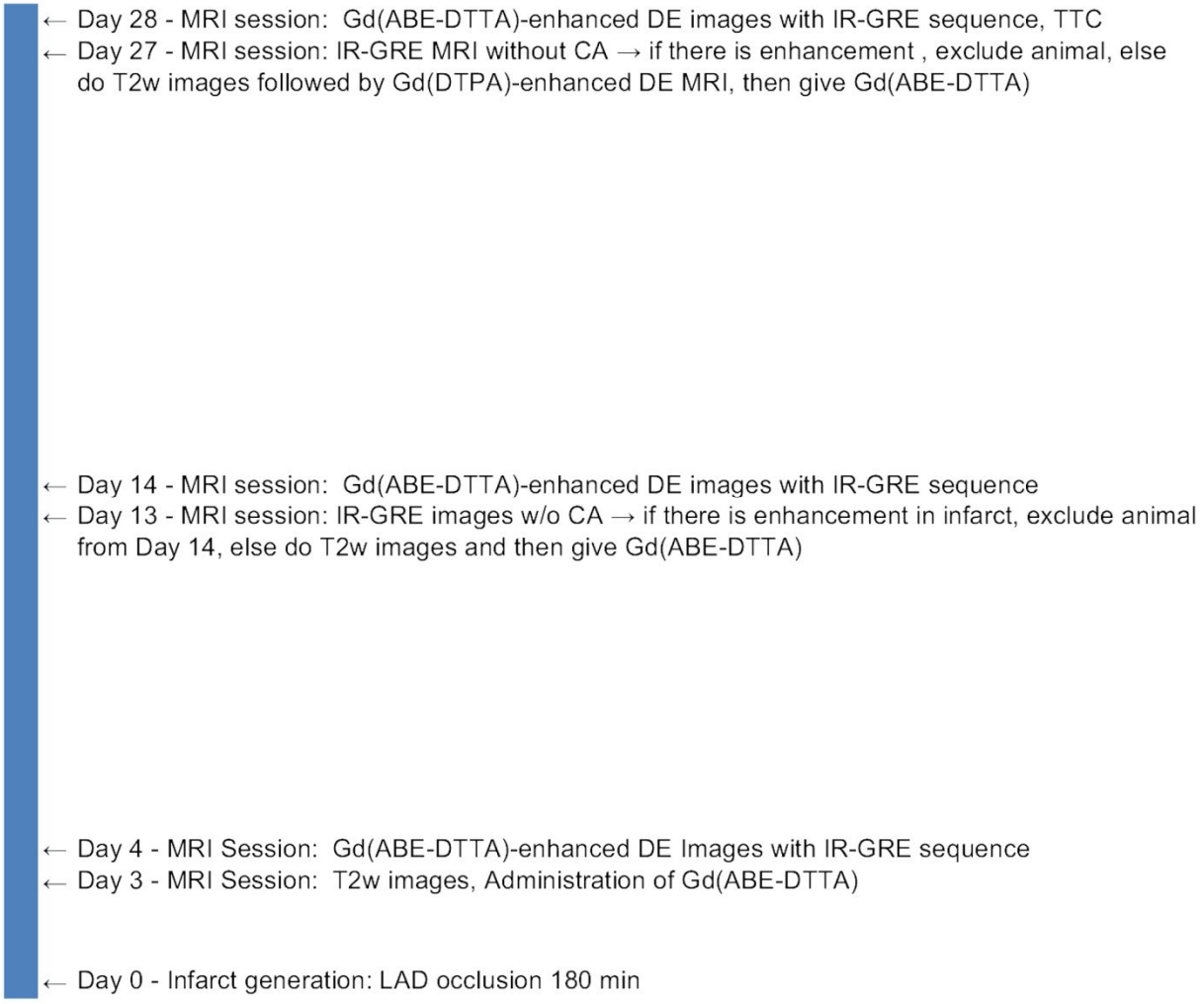


**Fig. 7 – Experimental design and timeline of events**

### 4.2.3 Surgical procedure

The animal protocol was approved by the IACUC of our institution in full compliance with the 'Guidelines for the Care and use for Laboratory Animals' (NIH). Seven male hounds (18-20 kg) were used. Twelve hours prior to procedure food was taken away and 325 mg Aspirin given. Hounds were anesthetized with a Ketamine (5.0mg/kg) and Diazepam (0.5mg/kg) mixture, intubated, and connected to a Hallowell EMC Model 2000 respirator (Pittsfield, MA, USA) operated with a tidal volume of 400 ml at a rate of 16 BPM. Anesthesia was maintained by

continuous flow of Isoflurane (2.5-3 volume %), and repeated Fentanyl (50-100ug I.V. every 30 minutes) administration. ECG electrodes were placed on the chest to record electrophysiological signs of myocardial ischemia and arrhythmias. Heart rate and blood oxygen saturation were monitored using a pulse-oxymeter with the probe placed on the animal's tongue. The left femoral artery was separated surgically and an arterial sheath (6-8 French) was inserted. An I.V. line was placed to administer infusion and drugs. Heparin (100 IU/kg) was given intravenously to maintain the activated clotting time (ACT) above 300 seconds. A properly sized 2-3 mm angioplasty balloon was introduced into the LAD under fluoroscopic guidance and inflated for 180 minutes to create MI. Thereafter, the balloon was deflated to restore coronary circulation. Fluoroscopic coronary angiography confirmed the onset of reperfusion after balloon deflation.

On day 3, 4, 13, 14, 27, and 28 following MI, animals were re-anesthetized as described above, and MRI studies performed. After the last MRI session, animals were sacrificed, hearts were excised and sliced (5 mm thick slices). TTC staining (2%, 37°C) was carried out to validate the existence of myocardial infarcts. Both sides of each TTC slice were digitally photographed.

### 4.2.4 Magnetic Resonance Imaging

A 1.5T GE Signa-Horizon CV/i scanner (Milwaukee, WI, USA) was used. A cardiac phased-array coil and ECG gating were employed. Breath-hold was performed using a manual switch on the respirator at end-expiration. A 180°-prepared, segmented, inversion-recovery fast gradient-echo (IR-FGE) pulse sequence was used with: Field of View (FOV) of 30 cm, Echo Time (TE) of 3.32 ms, Views per Segment of 16, Shot Length of 114.8 ms, Repetition Time (TR) two cardiac cycles (1100-1600 ms), slice thickness of 10 mm, Image Matrix of 256x256, Flip Angle of 25°, NEX of 1. The Inversion Time (TI) was optimized to null the signal in normal

myocardium. Double inversion-recovery (black-blood) fast-spin-echo images were generated at end-diastolic phase of the cardiac cycle with the following parameters: FOV of 30 cm, TE of 60 ms, Echo Train Length of 16, Shot Length of 140 ms, TR of two cardiac cycles (1100-1600 ms), Slice Thickness of 10 mm, Image Matrix of 256x256, Flip Angle of 90°, NEX of 1. Conventional cardiac angulation planes were set and short axis slices covering the entire LV were obtained (six slices per heart). The scan (breathhold at end-expiration) time per image was 15-20 s for DE-MRI or for T2w imaging. The total imaging time was around 6 min for both sequences.

### 4.2.5 Contrast Agent

In the MRI session on day 13, the IR-FGE sequence was used without CA administration. On day 27, a 0.2 mmol/kg Gd(DTPA) (Magnevist, Schering, Kenilworth, NJ) bolus was administered intravenously. DE images were acquired with the IR-FGE sequence 15-20 min thereafter. In the MRI sessions on days 4, 14, and 28, DE images were similarly obtained, 24h after i.v. administration of 0.05 mmol/kg Gd(ABE-DTTA).

### 4.2.6 Image analysis

MRI Dicom images were imported as image sequences with the use of ImageJ. In all images, the endo-, and epicardial contours were traced manually. Efforts were taken to avoid including any artificially high signal intensity (SI) due to inadequately suppressed slow flow within the left ventricular cavity space on T2w images. Large regions of interests, remote from the infarct, were selected to measure baseline SI ± SD of the healthy myocardium. All other analyses were automated to eliminate observer bias. In accordance with the literature [62], pixels with SI above the mean + 6 SD of the normal myocardium were regarded as “enhanced” pixels. A myocardial region was regarded as affected [79] when at least 10 connected pixels of the myocardium

revealed enhanced signal intensity. Regions of interest (ROIs) were drawn automatically (by ImageJ) around all areas of the affected pixels in every infarct-affected slice, and their mean SI was measured. If no 10 connected enhanced pixels were found in any slice of a DE image set, an ROI (~100 pixels) was placed in the center of infarcted (but unenhanced) myocardium based on TTC staining [80], and the mean SI was measured on the stored image. The mean percent SIE was computed by [63]:

$$SIE = 100 \times \frac{SI_i - SI_n}{SI_n}$$

where $SI_i$ and $SI_n$ were the mean signal intensity in infarct and normal myocardium, respectively.

### 4.2.7 Statistical analysis

Statistical analysis was carried out by SigmaStat (Version 2.03; SPSS Inc, Chicago, IL, USA) and SPSS (Release 13.0; SPSS Inc, Chicago, IL, USA). Results are reported as mean ± SD. One-way repeated measures analysis of variance was used to compare mean signal intensity enhancement (SIE) of DE images enhanced by Gd(ABE-DTTA) or by the T2 weighting sequence on the different days, since these data sets passed both the normality and the equality of variances tests. An overall significance ($P<0.05$) was established for rejecting the null hypothesis that the three groups are not different, therefore pairwise differences between the groups were assessed by using the Holm-Sidak method of adjustment for multiple comparisons. Two-way repeated measures analysis of variance was used to compare the SI values among experimental groups (factor 1: infarct vs. normal, factor 2: age of infarct). Although the test of normality failed in this data set, thanks to the equality of variances, the equality of group sizes, and the high power of the performed test (0.989 with $\alpha=0.05$), the assumption of the F test in the two-way ANOVA with repeated measures was not violated [64]. An overall significance ($P<0.05$) was established for rejecting the null hypothesis that the six groups are not different. Pairwise

differences between the groups were assessed by using the Holm-Sidak method of adjustment for multiple comparisons.

A value of $P<0.05$ was considered significant in all statistical tests.

### 4.3 Results

Gd(ABE-DTTA) highlighted the infarct in all cases on day 4, but not at all on day 14 or on day 28 following MI (see an example shown in Fig. 8). By days 13 and 27 post MI, the previously administered Gd(ABE-DTTA) completely cleared from the myocardium, including the infarct area. The mean ± SD signal intensity (SI) of infarcted myocardium in the presence of Gd(ABE-DTTA) significantly differed on day 4 from that of healthy myocardium (45 ± 16.0 vs. 10 ± 5.0, $P<0.05$), but it did not on day 14 (11 ± 9.4 vs. 10 ± 5.7, P=NS), nor on day 28 (7 ± 1.5 vs. 7 ± 2.4, P=NS) (Fig. 9.). The mean ± SD signal intensity enhancement (SIE) induced by Gd(ABE-DTTA) was 386±165% on day 4, significantly different from SIE on day 14 (9±20%), and on day 28 (12±18%) following MI ($P<0.05$). The last two mean values did not vary significantly (P=NS) between them. Gd(DTPA) highlighted the infarct in all cases on day 27, inducing a SIE value of 312±40%.

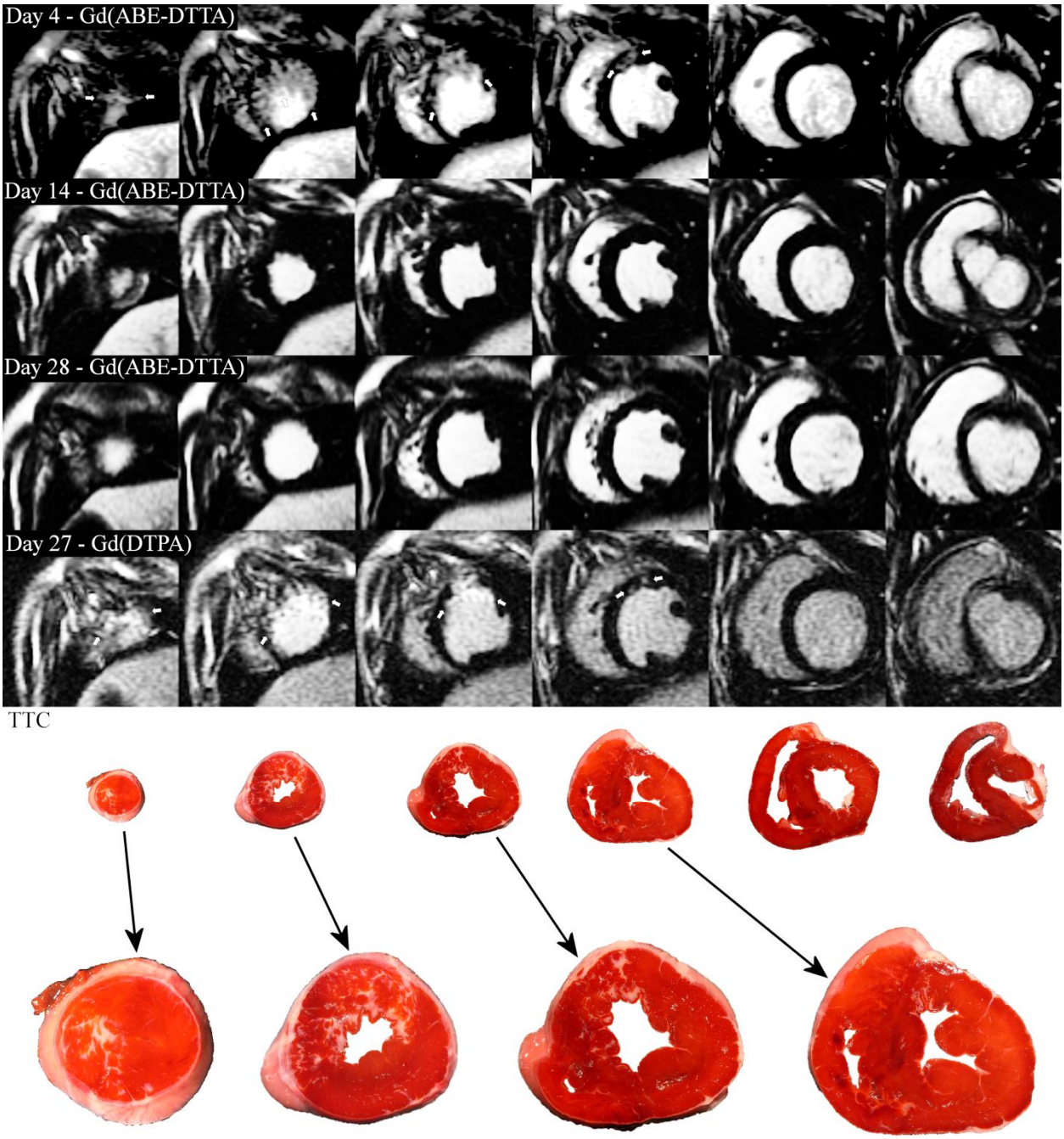


**Fig. 8 - Differentiation Between Acute vs. Subacute Myocardial Infarctions**

DE images taken in the presence of Gd(ABE-DTTA) on days 4, 14, and 28 after MI (panels 1 through 3 from top, respectively). Gd(ABE-DTTA) highlights the infarct on day 4 (see arrows), but does not on days 14 and 28. DE image set with Gd(DTPA) on day 27 (panel 4 from top). This image set ascertains that infarct is present (see arrows) despite the fact that it is not highlighted by Gd(ABE-DTTA) anymore. Corresponding TTC slices (panel 5 from top, and with increased size in panel 6 from top).

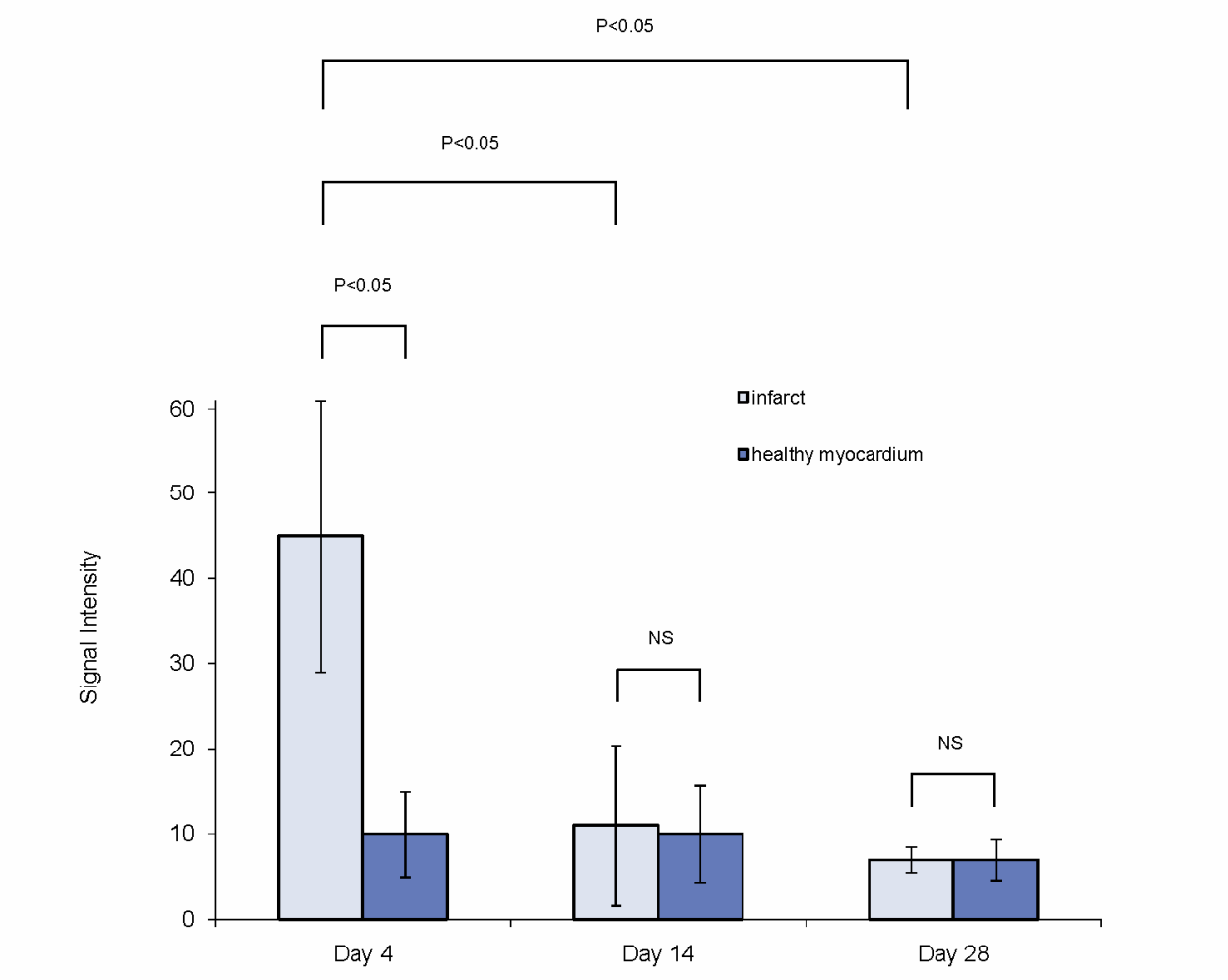


**Fig. 9 - Comparison of signal intensity values at Different Infarct Ages**

Mean (n=7) Signal Intensity values induced by Gd(ABE-DTTA) in areas of infarcts (bright blue bars) vs. healthy myocardium (dark blue bars) at different infarct ages. P values pertain to pairwise comparisons by the Holm-Sidak method of the six different experimental subgroups.

T2 weighted (T2w) signal enhancement was seen in the segments supplied by the infarct related artery (IRA) (Fig. 10). This enhancement appeared not only during the acute but also during the subacute and late subacute phase of the MI. The pattern of the enhancement was very similar in

these three different phases of scar healing. The mean ± SD SIE on day 3, 13, or 27 did not differ significantly (P=NS) on T2-TSE images (114±41%, 123±41%, and 150±79%, respectively). The existence of infarcts was also confirmed by TTC staining.

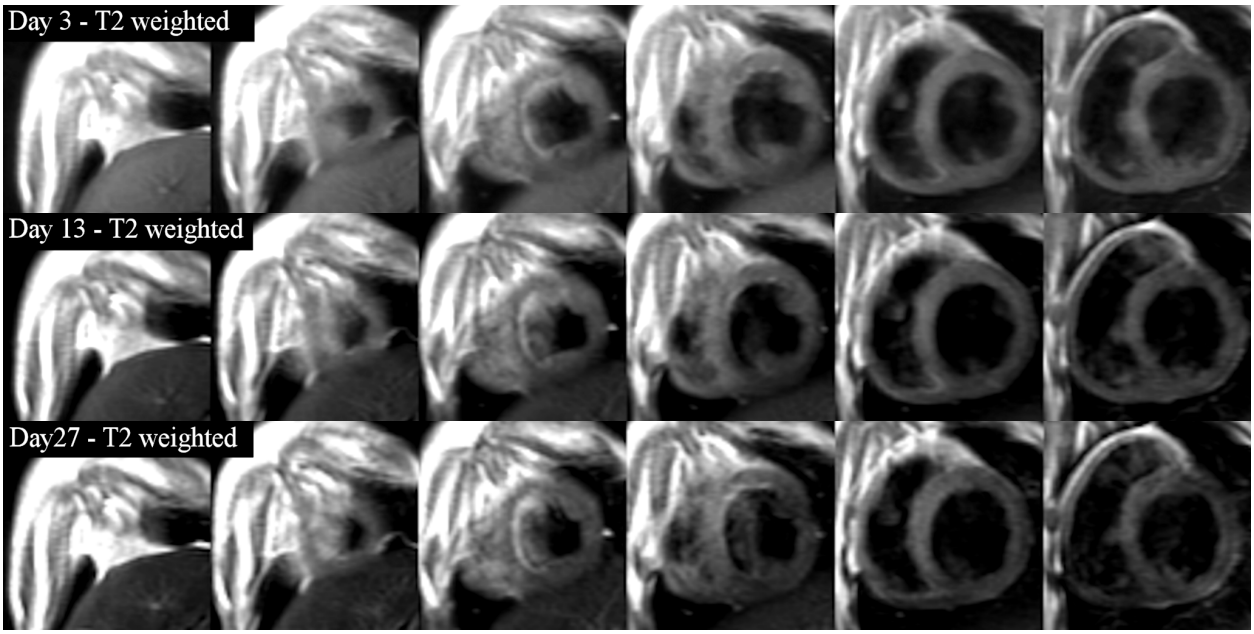


**Fig. 10 - T2w images**

Corresponding T2 weighted black-blood spin-echo images (TE=60 ms) of the same dog on Fig. 3 taken on days 3, 13, and 27 post MI (panels 1 through 3 from top, respectively). Note, that T2w signal enhancement can be observed in the anterior and anteroseptal segments not only during the acute but also during the subacute and late subacute phases of the myocardial infarct. The entire LAD-supply area (infarct related artery) is enhanced (area at risk), and not only the infarct- containing slices are involved. The pattern of the T2w-enhancement is quite the same in the 3 different phases of infarct scar healing.

## 4.4 Discussion

It had been shown earlier that Gd(ABE-DTTA) differentiates between acute and 4-week old myocardial infarcts (MI) in a canine, double infarct model [76, 77]. This previous model was designed to demonstrate the agent's ability to differentiate between acute and late subacute MIs in an animal having both types of myocardial infarct simultaneously. The principal finding of the current study is that Gd(ABE-DTTA) has a similar ability already at an earlier age of infarct, i.e.

14 days following MI. It shows that the infarct affinity of Gd(ABE-DTTA) has already vanished in the subacute phase of scar healing. This study also confirms the agent's ability to differentiate acute and older myocardial infarcts in an experimental study design different from the design in the previous study. It is also demonstrated, that T2w imaging highlights the infarcts and the segments supplied by the infarct-related artery ("area at risk") similarly in the acute, subacute and late subacute phase, i.e. T2w imaging is not able to distinguish among these different phases of the myocardial infarct healing during the time window the study uses while Gd(ABE-DTTA) does, using the animal model, phased-array coil, and pulse sequences described above.

To the best of our knowledge, similar results have not been obtained using any other MRI contrast agent or any other MRI method, capable of differentiating new myocardial infarcts from existing acute infarcts as early as in the subacute phase, achieving this with high sensitivity and specificity.

Several methods using cardiovascular MRI for differentiation between acute and older myocardial infarcts have been published, but none of them showed ability to differentiate an acute infarct from a subacute infarct, allowing its use for infarct age differentiation early on.

An intravascular, high molecular weight contrast agent, P792, Vistarem (Guerbet Group, Paris, France) was recently studied by Saeed et al. [65] at two different time-points in a single MI, in a porcine model. Vistarem induced hyperenhancement in the acute infarct but not in the later, chronic phase of MI. The authors have also demonstrated the superiority of their method over the T2-weighted (T2w) MRI technique for differentiation between acute and chronic MI. The significant difference from our current study was that Saeed at al. elucidated the affinity to MI of the CA in an advanced, chronic phase of scar healing, at *2 months* of infarct age.

Similarly, Abdel-Aty et al. [40] compared patients' MI in the acute vs. chronic phase. They combined Gd(DTPA)-induced DE with T2-weighted (T2w) MRI. T2-weighted MRI sequences are sensitive to water-bound protons. The distinction was based on an elevated T2w signal intensity due to infarct-related edema, which was expected to be present exclusively in the acute phase of MI [40]. Abdel-Aty et al. applied their method to compare with an older infarct than was investigated in our current study.

Kim et al. [68] used contrast enhanced steady state free precession (SSFP) MRI for the differentiation between acute and chronic (above *6 month old*) MIs in patients. Two minutes after Gd(DTPA) administration they observed elevated mean signal intensity in acute infarct areas with SSFP MRI. Chronic infarct regions, however, showed signal intensities similar to that of normal myocardium.

Our results showing that T2w imaging enhances the signal intensity in the territory of myocardial infarcts in subacute and late subacute infarcts are in accord with a previous publication of Johnstone at al. [81]. They found that the T2 relaxation time of the infarcted myocardium increased markedly at 3 days and remained elevated for 2 months in rabbits.

A 14 days old infarct is markedly different from a 28 days old infarct from the histological point of view. Richard et al. evaluated 14 day old myocardial infarcts [82] in a canine, reperfused model which were "characterized by a central core of persistent necrotic myocytes surrounded by an irregular rim of inflammatory cells, macrophages, and young scar (granulation tissue) composed of fibroblasts, new capillaries, and collagen". Histology samples taken from four week old myocardial infarcts of canines [76, 77], on the other hand, showed a more advanced stage of healing, with granulation tissue, collagen deposition, and small areas of interstitial fibrosis adjacent to the late subacute infarct. It is clear from these tissue differences that no extrapolations

could be made about the affinity of Gd(ABE-DTTA) to subacute infarct on the basis of results obtained in late subacute infarct, and that experimental comparison between the two was warranted. It also needs to be noted, from a potential clinical point of view, that MRI distinction between an acute and a subacute infarct would be of paramount importance for the in vivo validation of a pathological and clinical entity, the myocardial infarct extension. Infarct extension is defined clinically as an early in-hospital reinfarction after myocardial infarction, appearing in histology as acute foci of contraction band necrosis around a subacute infarct [83]. Until now, the in vivo verification of this pathological entity has not been possible with any imaging modality due to the lack of capability for differentiation between an acute and a subacute infarct.

The exact mechanism of the DE phenomenon is not known to date even for standard extracellular agents. Enlarged distribution volume due to sarcolemmal membrane rupture in acute infarcts and low grade of cellularity with expanded interstitial collagen matrix in chronic scar tissue have been suggested as potential mechanisms for infarct accumulation of such agents [35, 36, 53, 54, 69]. The exact mechanism of delayed enhancement effect induced by Gd(ABE-DTTA) is not known to date, either. The possible mechanisms [76, 77] may differ from that induced by standard extracellular CAs considering the different behaviour of the two agent types in subacute infarcts.

The differentiation shown by Gd(ABE-DTTA) on the basis of infarct age as early as in the subacute phase, indicates that this agent may become a reliable diagnostic tool in several important clinical situations, once it is approved for human application. The most important potential scenarios would be the following:

1. Localization of the "culprit" vessel in patients with multi-vessel CAD in acute NSTEMI in the presence of an old MI

In the course of a non-STEMI in patients with multi-vessel CAD, the determination of the culprit vessel could be challenging if the ECG is non-informative. In these cases, DE-MRI with standard extracellular contrast agents (eg. Gd(DTPA)) can localize the myocardial infarct (NSTEMI). If an older infarct is also present, Gd(DTPA) will highlight both the old and the new infarct. The additional use of Gd(ABE-DTTA) could selectively highlight the infarct corresponding with the culprit vessel. This could serve as a guide to the interventionalist for PCI.

2 . Detection of the extension of the myocardial infarct in its subacute phase.

Infarct extension is an event in the course of myocardial infarction [84] with serious short and long term consequences. It is defined clinically as an early in-hospital reinfarction after myocardial infarction. The pathologic finding of infarct extension is necrotic and healing myocardium with different recent (acute and subacute) ages within the same infarct territory [83]. Until now, the in vivo verification of this pathological event was not possible with any imaging modality due to the lack of capability for differentiation between an acute and a subacute infarct. Gd(ABE-DTTA), however, would be able to distinct between acute and subacute myocardial infarcts allowing the in vivo verification of extension of the myocardial infarct.

### 4.4.1 Study limitations

Our study has some limitations. Because of its special tissue kinetics properties, it is necessary to administer Gd(ABE-DTTA) ca. 24 hours before MRI imaging., This introduces an inconvenience, but not an unprecedented one, in a clinical setting.

## 4.5 Conclusions

In summary, we have shown that DE-MRI using Gd(ABE-DTTA) differentiates with high sensitivity and specificity between acute and 2-week-old (subacute) MI as it does between acute and 4-week old (late subacute) MI, in a reperfused, canine, single MI model. The infarct affinity of Gd(ABE-DTTA) vanishes as early as the subacute phase of scar healing.

This feature of Gd(ABE-DTTA) may become a reliable tool in several clinical situations, assuming the agent's approval for human application.

## 4.6 Acknowledgement

This study was partially supported by National Institutes of Health; Grant Number: 1R41 HL084844. An abstract of this work was presented at the 38th Annual Meeting of the North American Society of Cardiovascular Imaging (NASCI), October 3-5 2010, Seattle, Washington. A part of this work (the clinical implications paragraphs in the Discussion section) was presented at the 59th Annual Scientific Session of the American College of Cardiology, March 2010, Atlanta, Georgia.

# 5 Dobutamine stress cardiovascular magnetic resonance imaging in patients with peripheral artery disease

## 5.1 Introduction

Peripheral arterial disease (PAD) is a significant epidemiological problem by which 3278 percutane angioplasty (PTA) and 5101 amputations are implemented annually in Hungary [85]. Due to the systemic nature of the atherosclerosis and because of the typical existence of multiplex lesions, patients with peripheral arterial disease often have coronary heart disease as well, therefore the risk of coronary events is high. Most of the patients with PAD dies in consequence of his/her coronary artery disease [3]. Also very serious coronary artery disease can remain often asymptomatic because of the physical disability of the patient with PAD.

As it can be seen, the cardiology assessment of patients with PAD would be of great importance even if they do not have cardiac symptoms. However, their examination with conventional noninvasive cardiac tests is usually not possible or significantly limited because of the followings. Exercise ECG cannot be implemented due to the short intermittent claudication distance [46] of the patient. Patients with PAD often have chronic obstructive pulmonary disease (COPD) as a smoking related disease [47]. Therefore, basic hemodynamic measurements or assessment of wall motion abnormalities with transthoracic rest or stress echocardiography is often not possible or limited [48]. Dypiridamole or adenosine stress testing could be risky in patients with COPD and bronchospasm because of adverse reaction of these stressors [49-51]. Dobutamine stress MRI (DSMRI) which has grown to a clinically established test in the last two decades is able to identify patients with high risk for cardiac mortality and myocardial infarct [52]. This method based on the above detailed reasons enables the noninvasive assessment of severe coronary artery disease even in patients with PAD. The role of DSMRI, however, is

unknown to date in this patient population either from Hungarian or from international scientific literature. The aim of this study was to survey the safety and feasibility of DSMRI for the cardiac assessment of patients with PAD.

## 5.2 Patients and methods

### 5.2.1 Patients

The protocol of the study was approved by the Institutional Review Board of Flór Ferenc Hospital of Pest County and that of the Scientific Biomedical Committee. 21 patients (4 females, 17 males; mean ± SD age 64 ± 7.7 years) were enrolled after giving written informed consent. The patients were treated by the Flór Ferenc Hospital of Pest County because of PAD (ankle-brachial index 0.54 ± 0.18), and their medical history and current symptoms were negative from cardiology point of view. Patients having contraindications for MRI or administration of Dobutamine and/or Atropine [86, 87] were excluded from the study (Table 2).

**Table 2 - Exclusion criteria**

| |
|---|
| **Pacemaker non-compatible with MRI** |
| **Cardioverter defibrillator, neurostimulator** |
| **Starr-Edwards prosthetic valve** |
| **Intracranial aneurysm clips** |
| **Ear implants** |
| **Severe dyspnea at rest** |
| **Allergy to Dobutamine** |
| **Significant valvular heart disease** |
| **Hemodynamically relevant obstructive hypertrophic cardiomyopathy** |
| **Glaucoma** |
| **Claustrophobia** |
| **Restlessness** |
| **Atrial fibrillation** |

The main data of the patients can be seen in Table 3.

**Table 3 - Patient population**

| | |
|---|---|
| **Main characteristics of the patient population** | |
| **Sex (female, male)** | 4/17 |
| **Age, years** | 64±7,7 |
| **Body mass index, kg/m$^2$** | 26,4±4,4 |
| **Main clinical data** | |
| **Hypertension** | 17 (80,9%) |
| **Diabetes mellitus** | 7 (33,3%) |
| **Hyperlipoproteinaemia** | 13 (61,9%) |
| **Smoking** | 12 (57,1%) |
| **Arteriosclerosis in family history** | 12 (57,1%) |
| **Ankle/brachial index** | 0,54±0,18 |

### 5.2.2 MRI

Patients suspended their β-blocker treatment at least 24 hour before DSMRI. Blood pressure was measured by an automatic blood pressure monitor attached to a cuff with a long rubber tube. Systolic/diastolic blood pressure and heart rate were measured and documented in the beginning and in every 3 minuts of the examination. A catether was inserted into the cubital vein for later adminstration of Gadolinium-content MRI contrast agent and Dobutamine infusion (Atropine). Resustitation acquipment and defibrillator were installed at the entrance of the MRI scanner room. DSMRI was implemented in a group of the patients on a Vision Plus 1.5 T MRI scanner (Siemens, Erlangen Germany) (owner: Huniko Ltd., Miskolc, Hungary) in the Flor Ferenc Hospital of Pest County. The rest of patients was examined on a Signa Excite 1.5 T scanner

(General Electric Healthcare, Milwaukee, USA) owned by Raditec Ltd. (Budapest, Hungary). A six-element cardiac coil was used for signal acquisition. The synchronization of the acquisition was performed by triggering on the R wave of ECG lead by MRI compatible chest electrodes. The ECG served as a continuous monitor of heart rhythm at the same time. The acquisition was implemented in expiratory breath-hold.

The positioning of the patient in the scanner was followed by definition of cardiac axes using localizing images. For that purpose, rapid gradient echo sequence was used for Vision Plus and Fiesta sequence was applied for Signa Excite. The three typical planes (4 chamber, 3 chamber, 2 chamber views) were setup and cine images were acquired. For that purpose, gradient echo sequence was used for Vision Plus with these technical parameters: spatial resolution of 1.6 × 1.6 × 8 $mm^3$, repetition time (TR) of 80 ms, echo time (TE) of 4.8 ms, flip angle of 20°. The breath-hold time per slice was kept around 15 s. The prospective ECG gating pertaining to the used cine gradient echo acquisition sequence necessitated the continuous adjusting of number of phases acquired per heart cycle to the wide range of heart rates (50-150/min) during stress protocol. Cine MRI on Signa Excite was implemented by Fiesta sequence: spatial resolution of 1.6 × 1.6 × 8 $mm^3$, TR of 3.57 ms, TE of 1.58 ms, flip angle of 50°. This sequence uses retrospective gating, 20 phases per heart cycle were setup. Three short axis (basal, midventricular, apical) planes and at least one of the long axis planes were selected for further imaging. The cine MRI images acquired during every level of the stress protocol were setup in these planes. These planes covered the 17 segments of the entire left ventricle according to the recommendation of the American Heart Association for standardized myocardial segmentation and nomenclature in cardiac imaging [88]. Dobutamine hydrochloride was administered intravenously by a digital injector in doses of 10, 20, 30, and 40 μg/kg/min. New or worsened wall motion abnormalities as

well as image quality on the acquired cine images were continuously monitored. If segmental wall motion abnormalities were detected in rest, the stress was started at dose of 5 μg/kg/min of Dobutamine. This enabled to recognize hibernating myocardium hence the motion of the given segment improves at this dose of Dobutamine. In case of the lack of other reasons, the administration of Dobutamine was terminated if the age predicted target heart rate was reached. This was calculated by the formula of (220-age) × 0.85. If the target heart rate was not attained, additional intravenous Atropine boluses were given in 0.25 mg fractions in every 60 seconds up to 1 mg.

During stress, cine images were acquired using the aforementioned MRI sequences. Three short axis (basal, midventricular, apical) planes and at least one of the long axis planes were setup, the very same planes selected for the imaging in rest. ECG and the symptoms were continuously monitored and documented while the blood pressure and heart rate were recorded. Standard termination criteria were used [89, 90] (Table 4).

**Table 4 - Termination criteria before the target heart rate reached**

| |
|---|
| **New or worsening wall motion abnormalities** |
| **Decrease of systolic blood pressure >40 Hgmm** |
| **Significant (>240/120 mmHg) increase of systolic blood pressure** |
| **Serious chest pain** |
| **Severe dyspnoea** |
| **Impairment of global left ventricular function** |
| **Complex ventricular arrhythmias** |
| **Atrial fibrillation/flutter with high ventricular response** |
| **No tolerable side effects (nausea, vomitus)** |
| **Patient's request** |

The stress was followed by rest phase acquiring further cine images. The spontaneous relief of symptoms might occur during stress was facilitated by iv. metoprolol (5-10 mg). After Dobutamine stress, Gadopentane-dimeglumin (Magnevist, Bayer-Schering Pharma AG, Germany) was given. 10-15 min following contrast agent administration, late enhancement images were acquired. For that purpose, inversion recovery gradient echo sequence was used either for Vision Plus or for Signa Excite with the following parameters: spatial resolution of 1.6 × 1.6 × 8 $mm^3$, repetition time of 2 cardiac cycles (1100-1600 ms), echo time of 3.4 ms (Vision Plus) or 3.67 ms (Signa Excite), flip angle of 20°. The duration of breath holding was around 15 seconds for every slice.

### 5.2.3 Image analysis

MRI images were analysed independently by two experienced cardiologists having European CMR accreditation who were blinded to the clinical data of the patients. Left ventricular end diastolic and end systolic volume, the ejection fraction, and the left ventricular mass were determined by Segment v1.8 R1021 software (http://segment.heiberg.se) using the short axis slices. Endocardial borders on the end diastolic and end systolic images were contoured manually. Wall motion abnormalities were assessed on the screen in synchronized mode on three short axis and one long axis cine images acquired in different phases of the stress protocol applying standardized scoring system (1=normokinetic 2=hypokinetic 3= akinetic 4= dyskinetic) and the 17-segment model of the American Heart Association [88]. Reversible ischemia was defined as new wall-motion abnormality (increase of wall motion score) or bifasic response in segments with resting wall-motion abnormalities (increase of wall motion abnormality followed by re-decrease) appearing in ≥1 segment. The quality of images was rated

on a 4-point scale [91] based on the visibility of the endocardial border (1=poor or nondiagnostic; 2= partially or moderately visible; 3=good visibility; 4=excellently visible).

### 5.2.4 Statistical analysis

Statistical analysis was carried out using 15.0 Version of SPSS for Windows and 5.3 Version of SigmaStat for Windows (SPSS Inc., Chicago, USA). The normality of the distribution of different statistical variables was analyzed with Kolmogorov-Smirnoff test. Variables are reported as mean±SD if they passed the test of normality. Otherwise, they a reported as median with $25^{th}$ and $75^{th}$ percentiles shown in brackets [quartile]. Interobserver agreement for the assessment of wall motion abnormalities was determined by kappa test. Kruskal-Wallis analysis of variance for nonparametric variables was used for the analysis of the difference of median image quality scores between different anatomical regions. The statistical difference between median image quality scores at rest or during stress was evaluated by Wilcoxon signed-rank test. $P \leq 0.05$ was considered significant.

## 5.3 Results

### 5.3.1 Study group

Technical problems occurred rarely during MRI examinations. The setup of the EKG lead must have been changed in two patients (9.5%) for correct EKG-gating during stress conditions. Hemodynamic data of patients at rest and during stress are reported in Table 5.

**Table 5 - Hemodynamic data**

| | |
|---|---|
| **Left ventricular function (at rest)** | |
| **LVEF, %** | 71,2±9,3 |
| **LVEDV, ml** | 123,9±41,2 |
| **LVESV, ml** | 36,3±19,1 |
| **Heart rate, 1/min** | |
| **At rest** | 75,3±15,7 |
| **At maximal stress** | 134,5±12,1 |
| **Age predicted target heart rate** | 132,3±6,5 |
| **Heart rate reached in percent of target heart rate** | 101,7±8,4 |
| **Systolic blood pressure, mmHg** | |
| **At rest** | 140,9±16,1 |
| **At maximal stress** | 150,9±27,1 |
| **Diastolic blood pressure, mmHg** | |
| **At rest** | 81,4±5,7 |
| **At maximal stress** | 83,1±12,5 |
| **Heart rate x blood pressure, mmHg/min** | |
| **At rest** | 10625,4±2555,5 |
| **At maximal stress** | 20319,8±4049,1 |

The administration of Dobutamine must have been terminated before the age-predicted target heart rate was attained in one, otherwise symptomless patient (4.8%) because of decrease of blood pressure more than 40 mmHg from a previous level. The Dobutamine stress was terminated in the other 20 patients (95.2%) when the target heart rate was attained. Also the new wall motion abnormalities showed up always when the heart rate was reached. Dose of the Dobutamine at termination was 20 µg/kg/min body weight in 4 patients (19.0%), 30 µg/kg/min in 8 patients (38.1%), 40 µg/kg/min in 9 patients (42.9%). 2 patients needed additional 1 mg Atropine (0.25 mg bolus per minute) administration in order to attain the target heart rate. 11 patients (52,4%) did not have any symptoms during stress. One patient (4.8%) developed a

typical, but not severe angina pectoris. Mild chest discomfort showed up in four (19.0%), tachypnoe in one (4.8%), flush and itch of the skin in one (4.8%), palpitation in two (9.5%) studies. Tree patients (14.3%) had a couple of isolated ventricular premature beats. Administration of intravenous metoprolol following Dobutamine stress was necessary in five (23.8%) cases; four patients (19.0%) received 5 mg, one patient (4.8%) received 10 mg. Malignant ventricular rhythm disturbances, hemodynamic instability, serious angina or any other severe adverse event did not occur. 5 patients (23.8%) have an inducible wall motion abnormality during Dobutamine stress. Late enhancement was detectable in 5 cases (23.8%) of the studies. Dobutamine stress MRI examination of a patient can be seen as an example on Fig. 11.

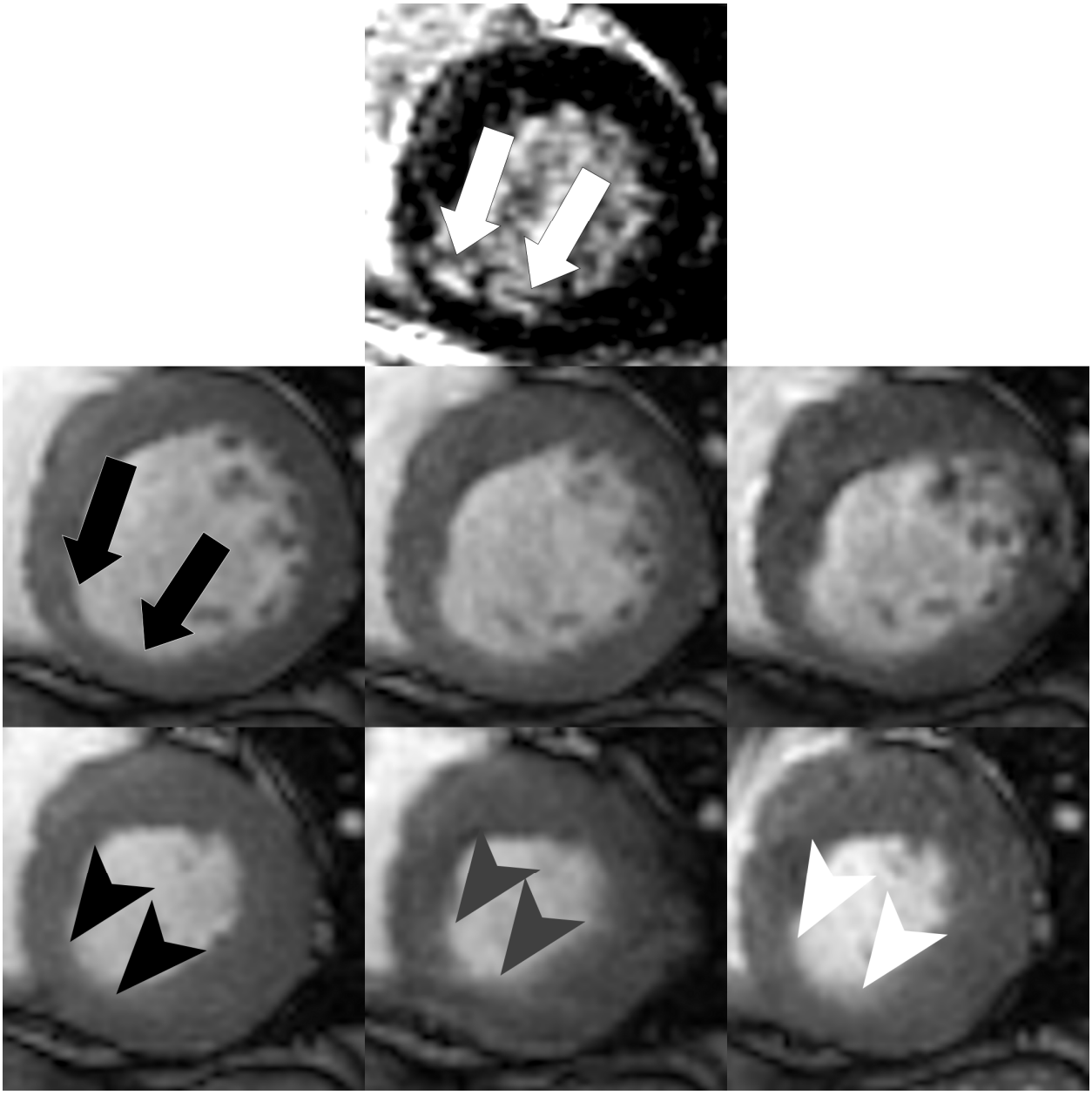

**Fig. 11 - DSMRI and LE examinations in a patient**

Basal short axis late enhancement (LE) CMR image can be seen in the top raw. White arrows show a subendocardial infarct on the border of inferior and inferoseptal segment. Corresponding cine SSFP images are seen in the enddiastolic (ED) (middle raw) and in the endsystolic (ES) phase (bottom raw). From left to right, rest, low dose (5μg/kg/min), and maximal (in this case 30 μg/kg/min) Dobutamine stress images are demonstrated, respectively. Black arrows show that the myocardium is thinned on the border between inferior and inferoseptal segment, according to the sebendocardial infarct. Black arrowheads show that this segment is hypokinetic at rest, hence the systolic wall thickening is significantly reduced. Sytolic wall thickening is improved at low dose (gray arrowheads), and decreased (white arrowheads) at maximal Dobutamine stress (biphasic response). Coronary angiography confirmed the occlusion of the right coronary artery (RCA). The occluded part of the RCA was supplied by homocoronary collateral anastomoses minimally.

### 5.3.2 Wall motion abnormalities and image quality

The interobserver agreement for the assessment of wall motion abnormalities was $\kappa$ =0,87 ($p<0,0001$). Median image quality score for all anatomical localizations was high (4 [4-4]) on the 4-point scale at rest or during stress. The apex (segment 17) has relatively the worth median image quality at rest (4 [3-4]), while all other segments have 4 [4-4]. Despite of that, the median image quality did not change significantly between different anatomical localizations (p=NS). There was no statistical difference (p=NS) between image quality of four anatomical regions (anterior, lateral, inferior, and septal) at rest or during stress, either.

## 5.4 Discussion

A number of publications have confirmed that Dobutamine stress MRI became a clinically established and generally used method for the noninvasive assessment of reversible myocardial ischemia [89, 92-100]. Publication of Nagel et al. [95] have proved that Dobutamine stress MRI detects reversible ischemia more precisely than Dobutamine stress echocardiography. The use of cardiac MRI versus echocardiography has been shown by the study of Nagel et al. to improve sensitivity from 74% to 86% while specificity from 70% to 86%. The superiority of cardiovascular MRI could be linked to its better overall image quality which was ranked good or very good in 82% while simply 51% of patients' examination with echocardiography [95]. Compared to other noninvasive methods, Dobutamine stress MRI could be useful for the assessment of patients suspected for ischemic heart disease [89]. To date, it has not been published any original papers concerning the feasibility and safety of Dobutamine stress MRI for the cardiac assessment of patients with PAD having high risk for cardiovascular morbidity and mortality. Serious adverse event did not occur during this study. It is in accord with other publications [89, 93, 94, 101-103] found Dobutamine stress MRI to be safe. Wahl et al. [101]

published the rate of occurrence of sustained ventricular tachycardia 0.1% while that of sustained ventricular tachycardia 0.4% in a population of 1000 patients. Side effects during stress in current study could be regarded to be negligible. A favorable ratio was also attained in the sense of age- predicted target heart rate during Dobutamine-atropine stress (95.2%). This ratio could be ranked good compared to the 85% experienced by Elhendy et al. [104] during treadmill stress of patients suspected for coronary artery disease. This difference could be noticed even more favorable if the claudication symptoms of the patient population examined in the current study is taken into account. The claudication could have limited significantly the maximal stress level attained during treadmill test.

The high median quality scores of the acquired images, the uniformity of the image quality scores of different anatomical regions and that of cine images acquired at rest versus during test equally show the feasibility of Dobutamine stress MRI in the studied population of patients. It has also been shown in this study that Dobutamine stress MRI provides excellent interobserver agreement for the assessment of wall motion abnormalities in patients with PAD which probably could be linked to the high image quality of the cine CMR images. Further advantage of the Dobutamine stress MRI is that the analysis of wall motion abnormities can be combined with other cardiovascular MRI technologies such as the Gadolinium late enhancement imaging of myocardial infarct scar. With this method, a relatively high rate (23.8%) of unknown myocardial infarct involving different percentage of the myocardial wall was detected. This information supplemented with that of response to Dobutamine stress MRI can help in the determination of salvageable myocardium if revascularization is to be made [31, 105]. Five patients (23.8%) have inducible wall motion abnormalities in study. Landesberg et al. [106] detected a similar rate of occurrence of reversible myocardial ischemia with preoperative Thallium Myocardium

Scintigraphy in patients with PAD. Compared to that, other publications [89, 95, 101] reported a higher rate (42-51-67%) of inducible wall motion abnormalities in patients with angina pectoris and suspected for coronary heart disease. The results of this study show that Dobutamine stress MRI for the noninvasive cardiac assessment of patients with PAD safe and feasible method.

# 6 Discussion

## 6.1 Determination of the Age of Myocardial Infarct

Differentiation between acute and older myocardial infarcts is of great importance in clinical decision-making. To date, differentiation between acute and older MIs represents a challenge for existing imaging modalities [40]. Standard extracellular contrast agents used with DE-MRI highlight both the acute and the chronic MI. Also, the magnitude of signal intensity enhancement is the same in the territory of a MI in the two stages [35, 41].

Our first study have shown that our method differentiates between acute and older myocardial infarct in a canine, double infarct model, using myocardial delayed-enhancement magnetic resonance imaging by a new MRI contrast agent developed in our laboratory. Gd(ABE-DTTA) was capable of differentiating between acute (four-day old) and late subacute (four-week old) infarcts. The first study was designed to demonstrate the agent's ability to differentiate between acute and late subacute MIs in an animal having both types of myocardial infarct simultaneously. In our second study, have confirmed that Gd(ABE-DTTA) has a similar ability already at an earlier age of infarct, i.e. 14 days following MI. Infarct affinity of Gd(ABE-DTTA) vanishes in the subacute phase of scar healing. The agent's ability has been shown to differentiate acute and older myocardial infarcts in an experimental study design different from the design in the first study. It has also been demonstrated, that conventionally used T2w imaging highlights the

infarcts and the segments supplied by the infarct-related artery ("area at risk") similarly in the acute, subacute and late subacute phase. It involves that T2w imaging is not able to distinguish among these different phases of the myocardial infarct healing during the time window the study uses while Gd(ABE-DTTA) does. These observations are in accord with a previous publication of Johnstone at al. [81]. They found that the T2 relaxation time of the infarcted myocardium increased markedly at 3 days and remained elevated for 2 months in rabbits.

Several methods using cardiovascular MRI for differentiation between acute and older myocardial infarcts have been published, but none of them showed ability to differentiate an acute infarct from a subacute infarct, allowing its use for infarct age differentiation early on [40, 65, 68].

The evolution of MI is a complex, dynamic pathohistological process [70] in which dead myocytes are removed and replaced by scar. Various rationales for the ability of Gd(ABE-DTTA) to selectively accumulate in acute myocardial infarct could be put forth, but they should be related to the different phases of the above healing process.

The first explanation could be linked to the partial intravascular nature [55] of Gd(ABE-DTTA). The partial intravascular nature means that in the case of normal microvascular endothelial structure, the agent penetrates into the extravascular space to a lesser extent than standard extracellular agents do. Microvascular damage in an acute infarct [70] could lead to increased microvascular permeability towards CAs with intravascular behavior [71, 72], while the remodeled microvessels in healing infarcts [65, 73] would reduce such permeability for an intravascular agent. Having partial intravascular characteristics [55], the above mentioned increased microvascular permeability in acute stage of the disease could augment locally the distribution volume of Gd(ABE-DTTA) in the infarct. This can lead to increased concentrations

of the agent in the infarcted tissue, ie. to the generation of hyperenhancement. The decline of the microvascular permeability in two-week old, or older, infarcts may result in diminished volume of distribution of this type of CA, and, therefore, to the disappearance of the hyperenhancement. The second explanation may be based on a possible necrosis-avidity of Gd(ABE-DTTA). Binding sites for the CA may exist among the different elements of acute necrotic tissue such as subcellular compartments (ruptured membrane, cytosol, mitochondria), calcium precipitates [70, 74] or ingredients of acute inflammatory reactions, persisting selectively in acutely infarcted tissue. The progressive, persistent [55] accumulation of Gd(ABE-DTTA) in acutely infarcted tissue may be partly due to its partial lipophilic nature [44], whereby lipids derived from the above mentioned cellular components may bind this CA. The existence of these presumed binding sides may be confined to the acute phase of myocardial infarct which could lead to acute-infarct selectivity of this CA. The two hypotheses are not mutually exclusive, as the combination of the two mechanisms could lead to the acute infarct selectivity demonstrated.

### 6.2 Detection of reversible ischemia with Dobutamine stress MRI in patients with PAD

We have discussed above, that examination of patients with PAD is often not possible or significantly limited with conventional noninvasive cardiac tests. A diagnostic imaging method for the cardiac assessment for these patients is warranted to identify those who are at high risk for undesirable cardiac events. DSMRI is able to identify patients with high risk for cardiac mortality and myocardial infarct [52] with high sensitivity and specificity. DSMRI permits the noninvasive assessment of severe coronary artery disease even in patients with PAD. Our third study has demonstrated that DSMRI is feasible with low risk for the cardiology assessment of patients with peripheral arterial disease.

The lack of serious adverse events during our third study is in accord with other publications [89, 93, 94, 101-103] found Dobutamine stress MRI to be safe. A favorable ratio of age-predicted target heart rate during Dobutamine-atropine stress (95.2%) was also attained compared to the 85% experienced by Elhendy et al. [104] during treadmill stress of patients suspected for coronary artery disease, especially if the claudication symptoms of the patient population examined in the current study is taken into account.

The high median quality scores of the acquired images, the uniformity of the image quality scores of different anatomical regions and that of cine images acquired at rest versus during test equally show the feasibility of Dobutamine stress MRI in our third study. It has also been shown that Dobutamine stress MRI provides excellent interobserver agreement for the assessment of wall motion abnormalities in patients with PAD which probably could be linked to the high image quality of the cine CMR images. 23.8% of the patients have inducible wall motion abnormalities. Landesberg et al. [106] detected a similar rate of occurrence of reversible myocardial ischemia with preoperative Thallium Myocardium Scintigraphy in patients with PAD. Compared to that, other publications [89, 95, 101] reported a higher rate (42-51-67%) of inducible wall motion abnormalities in patients with angina pectoris and suspected for coronary heart disease.

### 6.3 Conclusion

Efforts for the decrease of the incidence and case fatality of myocardial infarction are important determinants of the desired decline in coronary disease mortality. The better recognition of pathological processes of different tissues following myocardial infarct could contribute to these efforts. In many ways, cardiac MRI is capable for the in vivo assessment of the irreversibly injured myocardial tissue as well as of the ongoing pathological processes during the healing of

myocardial scar following myocardial infarct. The phenomenon of acute infarct selectivity of Gd(ABE-DTTA) described by our studies could initiate the research for the recognition of unknown aspects of the remodeling process post MI. The described method for the determination of the age of myocardial infarct may supply better quality of treatment as well as better outcome for patients following myocardial infarct, assuming the approval of the new contrast agent for human application.

Another important aspect for the decline of the mortality of cardiovascular disease could be the identification of patients without symptoms but having the highest risk for cardiovascular mortality. The cardiology assessment of patients with PAD would be of great importance even if they do not have cardiac symptoms. The results of our third study show that Dobutamine stress MRI for the noninvasive cardiac assessment of patients with PAD safe and feasible method.

# 7 NOVEL FINDINGS

In the first series of our investigations we have proven that Delayed enhancement MRI with separate administrations of standard extracellular contrast agent, Gd(DTPA), and a new low molecular weight contrast agent, Gd(ABE-DTTA), differentiates between acute and late subacute infarct in a reperfused, double infarct, canine model. It has also been shown that Gd(ABE-DTTA) induces approximately the same SIE in acute infarcts as Gd(DTPA) does.

We have four new observations in the study:

1. In canines, with Gd(ABE-DTTA), the mean signal intensity enhancement (SIE) is significantly higher in the acute phase of infarct than in the four-week old infarct in a reperfused, double infarct model.

2. With Gd(ABE-DTTA), the mean signal intensity enhancement in four-week old infarct does not differ significantly from that of in healthy myocardium.

3. Gd(DTPA) produces similar signal intensity enhancements in acute and four-week old infarcts, i.e. the two values does not differ statistically significant.

4. The signal intensity enhancement in acute or 4 week old myocardial infarct induced by Gd(DTPA) is not different statistically from Gd(ABE-DTTA)-induced SIE in acute infarct.

In the second series of our investigations we have shown Gd(ABE-DTTA) differentiates similarly between acute and 2-week-old MI as it does between acute and 4-week old MI using DE-MRI in a reperfused, single myocardial infarct, canine model. Thus it is evident that the infarct affinity of Gd(ABE-DTTA) disappears already in the subacute phase of scar healing, allowing the use of this agent for infarct age differentiation early on, immediately following the acute phase. This study confirms the agent's ability to differentiate acute and older myocardial infarcts also in a different experimental study design. Conventional T2w imaging highlights the infarcts and the segments supplied by the infarct-related artery ("area at risk") similarly in the acute, subacute and late subacute phase, i.e. we have also demonstrated that T2w imaging is not able to distinguish among these different phases of the myocardial infarct healing during the time window the study uses while Gd(ABE-DTTA) does, using the animal model, phased-array coil, and pulse sequences described above.

The sensitivity and specificity of the method is high. We have four new observations in the study:

1. In canines, on day 4, the mean signal intensity (SI) of infarcted myocardium in the presence of Gd(ABE-DTTA) differs significantly from that of healthy myocardium, but it

does not on day 14, nor on day 28 following myocardial infarct in a reperfused, single infarct model.

2. The mean signal intensity enhancement (SIE) induced by Gd(ABE-DTTA) on day 4 differs significantly from mean SIE on day 14, and from mean SIE on day 28 following MI.

3. The mean SIE values induced by Gd(ABE-DTTA) on day 14 and on day 28 do not differ significantly between them.

4. The mean ± SD SIE on day 3, 13, or 27 do not differ significantly (P=NS) on T2-TSE images.

In the third series of our investigations we have shown that Dobutamine stress MRI for the noninvasive cardiac assessment of patients with PAD is a safe and feasible method.

We have seven new observations in the prospective study of 21 patients with peripheral artery disease with dobutamine stress cardiovascular MRI:

1. The interobserver agreement for the assessment of wall motion abnormalities is almost perfect.

2. Median [interquartile range] image quality score for all anatomical localizations is excellent (4 [4-4]) on the 4-point scale either at rest or during stress.

3. The median image quality does not change significantly between different anatomical localizations (P=NS).

4. There is no statistical difference between image quality of four anatomical regions (anterior, lateral, inferior, and septal) at rest or during stress (P=NS).

5. The protocol of the study is completed by a significant number of the patients.

6. The target heart rate is attained in a high proportion of the studies.
7. The side effects can be regarded to be acceptable, and serious adverse events are rare.

# 8 REFERENCES


1. Roger VL: **Epidemiology of myocardial infarction.** *Med Clin North Am* 2007, **91:**537-552; ix.
2. Kalra M, Gloviczki P, Bower TC, Panneton JM, Harmsen WS, Jenkins GD, Stanson AW, Toomey BJ, Canton LG: **Limb salvage after successful pedal bypass grafting is associated with improved long-term survival.** *J Vasc Surg* 2001, **33:**6-16.
3. Meskó É: **Arteriosclerosis obliterans.** In *Vascularis Medicina.* Edited by Meskó É. Budapest: Therapia Kiadó; 2004: 188-192
4. Carlos FGCG, Sophie L: **Classification and basic properties of contrast agents for magnetic resonance imaging.** *Contrast Media & Molecular Imaging* 2009, **4:**1-23.
5. Merbach AE, Toth E: *The Chemistry of Contrast Agents in Medical Magnetic Resonance Imaging.* Wiley; 2001.
6. Braunwald E: **Myocardial reperfusion, limitation of infarct size, reduction of left ventricular dysfunction, and improved survival. Should the paradigm be expanded?** *Circulation* 1989, **79:**441-444.
7. Stillman A, Oudkerk M, Bluemke D, Bremerich J, Esteves F, Garcia E, Gutberlet M, Hundley W, Jerosch-Herold M, Kuijpers D, et al: **Assessment of acute myocardial infarction: current status and recommendations from the North American society for cardiovascular imaging and the European society of cardiac radiology.** *The International Journal of Cardiovascular Imaging (formerly Cardiac Imaging)* 2011, **27:**7-24.
8. Whitman G, Kieval R, Wetstein L, Seeholzer S, McDonald G, Harken A: **The relationship between global myocardial ischemia, left ventricular function, myocardial redox state, and high energy phosphate profile. A phosphorous-31 nuclear magnetic resonance study.** *Journal of Surgical Research* 1983, **35:**332-339.
9. Reimer KA, Lowe JE, Rasmussen MM, Jennings RB: **The wavefront phenomenon of ischemic cell death. 1. Myocardial infarct size vs duration of coronary occlusion in dogs.** *Circulation* 1977, **56:**786-794.
10. Reimer K, Jennings R: **The "wavefront phenomenon" of myocardial ischemic cell death. II. Transmural progression of necrosis within the framework of ischemic bed size (myocardium at risk) and collateral flow.** *Lab Invest* 1979, **40:**633-644.
11. Burke AP, Virmani R: **Pathophysiology of Acute Myocardial Infarction.** *Medical Clinics of North America* 2007, **91:**553-572.
12. Verma S, Fedak PW, Weisel RD, Butany J, Rao V, Maitland A, Li RK, Dhillon B, Yau TM: **Fundamentals of reperfusion injury for the clinical cardiologist.** *Circulation* 2002, **105:**2332-2336.
13. Ambrosio G, Weisman H, Mannisi J, Becker L: **Progressive impairment of regional myocardial perfusion after initial restoration of postischemic blood flow.** *Circulation* 1989, **80:**1846-1861.
14. Rochitte CE, Lima JAC, Bluemke DA, Reeder SB, McVeigh ER, Furuta T, Becker LC, Melin JA: **Magnitude and Time Course of Microvascular Obstruction and Tissue Injury After Acute Myocardial Infarction.** *Circulation* 1998, **98:**1006-1014.
15. Jennings R, Schaper J, Hill M, Steenbergen C, Jr, Reimer K: **Effect of reperfusion late in the phase of reversible ischemic injury. Changes in cell volume, electrolytes, metabolites, and ultrastructure.** *Circ Res* 1985, **56:**262-278.

16. Johnston DL, Brady TJ, Ratner AV, Rosen BR, Newell JB, Pohost GM, Okada RD: **Assessment of myocardial ischemia with proton magnetic resonance: effects of a three hour coronary occlusion with and without reperfusion.** *Circulation* 1985, **71:**595-601.
17. Johnston D, Liu P, Rosen B, Levine R, Beaulieu P, Brady T, Okada R: **In vivo detection of reperfused myocardium by nuclear magnetic resonance imaging.** *J Am Coll Cardiol* 1987, **9:**127-135.
18. Asanuma T, Tanabe K, Ochiai K, Yoshitomi H, Nakamura K, Murakami Y, Sano K, Shimada T, Murakami R, Morioka S, Beppu S: **Relationship Between Progressive Microvascular Damage and Intramyocardial Hemorrhage in Patients With Reperfused Anterior Myocardial Infarction : Myocardial Contrast Echocardiographic Study.** *Circulation* 1997, **96:**448-453.
19. Ochiai K, Shimada T, Murakami Y, Ishibashi Y, Sano K, Kitamura J, Inoue S, Murakami R, Kawamitsu H, Sugimura K: **Hemorrhagic myocardial infarction after coronary reperfusion detected in vivo by magnetic resonance imaging in humans: prevalence and clinical implications.** *J Cardiovasc Magn Reson* 1999, **1:**247-256.
20. Fishbein M, Y-Rit J, Lando U, Kanmatsuse K, Mercier J, Ganz W: **The relationship of vascular injury and myocardial hemorrhage to necrosis after reperfusion.** *Circulation* 1980, **62:**1274-1279.
21. Shishido T, Beppu S, Matsuda H, Yutani C, Miyatake K: **Extension of Hemorrhage After Reperfusion of Occluded Coronary Artery: Contrast Echocardiographic Assessment in Dogs.** *Journal of the American College of Cardiology* 1997, **30:**585-591.
22. Bogaert J, Dymarkowski S, Taylor A: *Clinical Cardiac MRI.* Berlin Heidelberg: Springer; 2005.
23. Nagel E, Van Rossum AC, Fleck E: *Cardiovascular Magnetic Resonance.* Berlin Amsterdam: Springer; 2005.
24. Pérez-Mayoral E, Negri V, Soler-Padrós J, Cerdán S, Ballesteros P: **Chemistry of paramagnetic and diamagnetic contrast agents for Magnetic Resonance Imaging and Spectroscopy: pH responsive contrast agents.** *European Journal of Radiology* 2008, **67:**453-458.
25. Banci L, Bertini I, Luchinat C: *Nuclear and Electronic Relaxation.* VCH:Weinheim; 1991.
26. Weinmann HJ, Brasch RC, Press WR, Wesbey GE: **Characteristics of gadolinium-DTPA complex: a potential NMR contrast agent.** *AJR Am J Roentgenol* 1984, **142:**619-624.
27. Parmelee DJM, Walovitch RCP, Ouellet HSB, Lauffer RBP: **Preclinical Evaluation of the Pharmacokinetics, Biodistribution, and Elimination of MS-325, a Blood Pool Agent for Magnetic Resonance Imaging.** *Investigative Radiology* 1997, **32:**741-747.
28. Caravan P, Comuzzi C, Crooks W, McMurry TJ, Choppin GR, Woulfe SR: **Thermodynamic stability and kinetic inertness of MS-325, a new blood pool agent for magnetic resonance imaging.** *Inorg Chem* 2001, **40:**2170-2176.
29. Dewey M, Kaufels N, Laule M, Schnorr J, Wagner S, Kivelitz D, Raynaud J, Robert P, Hamm B, Taupitz M: **Assessment of myocardial infarction in pigs using a rapid clearance blood pool contrast medium.** *Magn Reson Med* 2004, **51:**703-709.
30. Peukert D, Kaufels N, Laule M, Schnorr Jr, Carme S, Farr T, SchÃ¶nenberger E, Taupitz M, Hamm B, Dewey M: **Improved Evaluation of Myocardial Perfusion and Viability With the Magnetic Resonance Blood Pool Contrast Agent P792 in a Nonreperfused Porcine Infarction Model.** *Investigative Radiology* 2007, **42:**248-255

31. Kim RJ, Wu E, Rafael A, Chen EL, Parker MA, Simonetti O, Klocke FJ, Bonow RO, Judd RM: **The use of contrast-enhanced magnetic resonance imaging to identify reversible myocardial dysfunction.** *N Engl J Med* 2000, **343:**1445-1453.
32. Haas F, Haehnel C, Picker W, Nekolla S, Martinoff S, Meisner H, Schwaiger M: **Preoperative positron emission tomographic viability assessment and perioperative and postoperative risk in patients with advanced ischemic heart disease.** *J Am Coll Cardiol* 1997, **30:**1693-1700.
33. Higgins CB, de Roos A: *MRI and CT of the Cardiovascular System.* Philadelphia: Lippincott Williams &Wilkins; 2006.
34. Setser R, Bexell D, O'Donnell T, Stillman A, Lieber M, Schoenhagen P, White R: **Quantitative assessment of myocardial scar in delayed enhancement magnetic resonance imaging.** *J Magn Reson Imaging* 2003, **18:**434-441.
35. Kim RJ, Fieno DS, Parrish TB, Harris K, Chen EL, Simonetti O, Bundy J, Finn JP, Klocke FJ, Judd RM: **Relationship of MRI delayed contrast enhancement to irreversible injury, infarct age, and contractile function.** *Circulation* 1999, **100:**1992-2002.
36. Fieno DS, Kim RJ, Chen EL, Lomasney JW, Klocke FJ, Judd RM: **Contrast-enhanced magnetic resonance imaging of myocardium at risk: distinction between reversible and irreversible injury throughout infarct healing.** *J Am Coll Cardiol* 2000, **36:**1985-1991.
37. Udvarhelyi IS, Gatsonis C, Epstein AM, Pashos CL, Newhouse JP, McNeil BJ: **Acute myocardial infarction in the Medicare population. Process of care and clinical outcomes.** *JAMA* 1992, **268:**2530-2536.
38. Elhendy A, Schinkel AFL, van Domburg RT, Bax JJ, Poldermans D: **Differential prognostic significance of peri-infarction versus remote myocardial ischemia on stress technetium-99m sestamibi tomography in patients with healed myocardial infarction.** *The American Journal of Cardiology* 2004, **94:**289-293.
39. De Luca G, Suryapranata H, Stone G, Antoniucci D, Biondi-Zoccai G, Kastrati A, Chiariello M, Marino P: **Coronary stenting versus balloon angioplasty for acute myocardial infarction: a meta-regression analysis of randomized trials.** *Int J Cardiol* 2008, **126:**37-44.
40. Abdel-Aty H, Zagrosek A, Schulz-Menger J, Taylor AJ, Messroghli D, Kumar A, Gross M, Dietz R, Friedrich MG: **Delayed Enhancement and T2-Weighted Cardiovascular Magnetic Resonance Imaging Differentiate Acute From Chronic Myocardial Infarction.** *Circulation* 2004, **109:**2411-2416.
41. Fieno DS, Hillenbrand HB, Rehwald WG, Harris KR, Decker RS, Parker MA, Klocke FJ, Kim RJ, Judd RM: **Infarct resorption, compensatory hypertrophy, and differing patterns of ventricular remodeling following myocardial infarctions of varying size.** *Journal of the American College of Cardiology* 2004, **43:**2124-2131.
42. Kim SK, Pohost GM, Elgavish GA: **Fatty-acyl iminopolycarboxylates: lipophilic bifunctional contrast agents for NMR imaging.** *Magn Reson Med* 1991, **22:**57-67.
43. Chu WJ, Simor T, Elgavish GA: **In vivo characterization of Gd(BME-DTTA), a myocardial MRI contrast agent: tissue distribution of its MRI intensity enhancement, and its effect on heart function.** *NMR in Biomedicine* 1997, **10:**87-92.
44. Saab-Ismail NH, Simor T, Gaszner B, Lorand T, Szollosy M, Elgavish GA: **Synthesis and in vivo evaluation of new contrast agents for cardiac MRI.** *J Med Chem* 1999, **42:**2852-2861.

45. Simor T, Chu WJ, Johnson L, Safranko A, Doyle M, Pohost GM, Elgavish GA: **In vivo MRI visualization of acute myocardial ischemia and reperfusion in ferrets by the persistent action of the contrast agent Gd (BME-DTTA).** *Circulation* 1995, **92:**3549-3559.
46. Collins EG, Langbein WE, Orebaugh C, Bammert C, Hanson K, Reda D, Edwards LC, Littooy FN: **Cardiovascular training effect associated with polestriding exercise in patients with peripheral arterial disease.** *J Cardiovasc Nurs* 2005, **20:**177-185.
47. Harris M: **A smoking related triad: PAD, COPD and CCF.** *Aust Fam Physician* 2004, **33:**207-210.
48. Attenhofer Jost CH, Jenni R: **[Stress echocardiography--principles, methodology, results and indications].** *Ther Umsch* 1997, **54:**698-710.
49. Burkhart KK: **Respiratory failure following adenosine administration.** *The American Journal of Emergency Medicine* 1993, **11:**249-250.
50. Eagle KA, Boucher CA: **Intravenous dipyridamole infusion causes severe bronchospasm in asthmatic patients.** *Chest* 1989, **95:**258-259.
51. Ottervanger JP, Haan D, Gans SJ, Hoorntje JC, Stricker BH: **[Bronchospasm, apnea and heart arrest following dipyridamole perfusion scintigraphy].** *Ned Tijdschr Geneeskd* 1993, **137:**142-143.
52. Korosoglou G, Elhmidi Y, Steen H, Schellberg D, Riedle N, Ahrens J, Lehrke S, Merten C, Lossnitzer D, Radeleff J, et al: **Prognostic value of high-dose dobutamine stress magnetic resonance imaging in 1,493 consecutive patients: assessment of myocardial wall motion and perfusion.** *J Am Coll Cardiol* 2010, **56:**1225-1234.
53. Mahrholdt H, Wagner A, Holly TA, Elliott MD, Bonow RO, Kim RJ, Judd RM: **Reproducibility of Chronic Infarct Size Measurement by Contrast-Enhanced Magnetic Resonance Imaging.** *Circulation* 2002, **106:**2322-2327.
54. Choi KM, Kim RJ, Gubernikoff G, Vargas JD, Parker M, Judd RM: **Transmural extent of acute myocardial infarction predicts long-term improvement in contractile function.** *Circulation* 2001, **104:**1101-1107.
55. Suranyi P, Kiss P, Ruzsics B, Brott BC, Simor T, Elgavish A, Baker RA, Saab-Ismail NH, Elgavish GA: **In vivo myocardial tissue kinetics of Gd(ABE-DTTA), a tissue-persistent contrast agent.** *Magn Reson Med* 2007, **58:**55-64.
56. Ruzsics B, Surányi P, Kiss P, Brott B, Elgavish A, Saab-Ismail N, Simor T, Elgavish G: **Gd(ABE-DTTA), a Novel Contrast Agent, at the MRI-Effective Dose Shows Absence of Deleterious Physiological Effects in Dogs.** *Pharmacology* 2006, **77:**188-194.
57. Simor T, Gaszner B, Oshinski JN, Waldrop SM, Pettigrew RI, Horvath IG, Hild G, Elgavish GA: **Gd(ABE-DTTA)-enhanced cardiac MRI for the diagnosis of ischemic events in the heart.** *J Magn Reson Imaging* 2005, **21:**536-545.
58. Kiss P, Suranyi P, Simor T, Saab-Ismail NH, Elgavish A, Hejjel L, Elgavish GA: **In vivo R1-enhancement mapping of canine myocardium using ceMRI with Gd(ABE-DTTA) in an acute ischemia-reperfusion model.** *J Magn Reson Imaging* 2006, **24:**571-579.
59. Suranyi P, Kiss P, Brott BC, Simor T, Elgavish A, Ruzsics B, Saab-Ismail NH, Elgavish GA: **Percent infarct mapping: an R1-map-based CE-MRI method for determining myocardial viability distribution.** *Magn Reson Med* 2006, **56:**535-545.
60. Ruzsics B, Suranyi P, Kiss P, Brott BC, Elgavish A, Simor T, Elgavish GA: **Head-to-head comparison between delayed enhancement and percent infarct mapping for assessment of myocardial infarct size in a canine model.** *J Magn Reson Imaging* 2008, **28:**1386-1392.

61. Donald WM: **An Algorithm for Least-Squares Estimation of Nonlinear Parameters.** *SIAM Journal on Applied Mathematics* 1963, **11:**431-441.
62. Beek AM, Bondarenko O, Afsharzada F, van Rossum AC: **Quantification of late gadolinium enhanced CMR in viability assessment in chronic ischemic heart disease: a comparison to functional outcome.** *J Cardiovasc Magn Reson* 2009, **11:**6.
63. Simonetti OP, Kim RJ, Fieno DS, Hillenbrand HB, Wu E, Bundy JM, Finn JP, Judd RM: **An improved MR imaging technique for the visualization of myocardial infarction.** *Radiology* 2001, **218:**215-223.
64. Witte RS, Witte JS: *Statistics.* 5th edn. Fort Worth: Harcourt Brace College Publishers; 1997.
65. Saeed M, Weber O, Lee R, Do L, Martin A, Saloner D, Ursell P, Robert P, Corot C, Higgins CB: **Discrimination of myocardial acute and chronic (scar) infarctions on delayed contrast enhanced magnetic resonance imaging with intravascular magnetic resonance contrast media.** *J Am Coll Cardiol* 2006, **48:**1961-1968.
66. Hillenbrand HB, Becker LC, Kharrazian R, Hu K, Rochitte CE, Kim RJ, Chen EL, Ertl G, Hruban RH, Lima JA: **23Na MRI combined with contrast-enhanced 1H MRI provides in vivo characterization of infarct healing.** *Magn Reson Med* 2005, **53:**843-850.
67. Nilsson JC, Nielsen G, Groenning BA, Fritz-Hansen T, Sondergaard L, Jensen GB, Larsson HB: **Sustained postinfarction myocardial oedema in humans visualised by magnetic resonance imaging.** *Heart* 2001, **85:**639-642.
68. Kim KA, Seo JB, Do KH, Heo JN, Lee YK, Song JW, Lee JS, Song KS, Lim TH: **Differentiation of recently infarcted myocardium from chronic myocardial scar: the value of contrast-enhanced SSFP-based cine MR imaging.** *Korean J Radiol* 2006, **7:**14-19.
69. Kim RJ, Chen EL, Lima JA, Judd RM: **Myocardial Gd-DTPA Kinetics Determine MRI Contrast Enhancement and Reflect the Extent and Severity of Myocardial Injury After Acute Reperfused Infarction.** *Circulation* 1996, **94:**3318-3326.
70. Fishbein MC, Maclean D, Maroko PR: **The histopathologic evolution of myocardial infarction.** *Chest* 1978, **73:**843-849.
71. Krombach GA, Wendland MF, Higgins CB, Saeed M: **MR Imaging of Spatial Extent of Microvascular Injury in Reperfused Ischemically Injured Rat Myocardium: Value of Blood Pool Ultrasmall Superparamagnetic Particles of Iron Oxide.** *Radiology* 2002, **225:**479-486.
72. Saeed M, van Dijke CF, Mann JS, Wendland MF, Rosenau W, Higgins CB, Brasch RC: **Histologic confirmation of microvascular hyperpermeability to macromolecular MR contrast medium in reperfused myocardial infarction.** *J Magn Reson Imaging* 1998, **8:**561-567.
73. Ren G, Michael LH, Entman ML, Frangogiannis NG: **Morphological characteristics of the microvasculature in healing myocardial infarcts.** *J Histochem Cytochem* 2002, **50:**71-79.
74. Marchal G, Ni Y, Herijgers P, Flameng W, Petre C, Bosmans H, Yu J, Ebert W, Hilger C, Pfefferer D, et al: **Paramagnetic metalloporphyrins: infarct avid contrast agents for diagnosis of acute myocardial infarction by MRI.** *Eur Radiol* 1996, **6:**2-8.
75. Vesely MR, Dilsizian V: **Nuclear Cardiac Stress Testing in the Era of Molecular Medicine.** *J Nucl Med* 2008, **49:**399-413.
76. Kirschner R, Varga-Szemes A, Toth L, Simor T, Suranyi P, Ruzsics B, Kiss P, Toth A, Baker R, Brott BC, et al: **Reinfarction-Specific Magnetic Resonance Imaging Contrast Agent.** *Journal of the American College of Cardiology* 2010, **55:**A84.E795-A784.E795.

77. Kirschner R, Toth L, Varga-Szemes A, Simor T, Suranyi P, Kiss P, Ruzsics B, Toth A, Baker R, Brott B, et al: **Differentiation of acute and four-week old myocardial infarct with Gd(ABE-DTTA)-enhanced CMR.** *Journal of Cardiovascular Magnetic Resonance* 2010, **12:**22.
78. Ruzsics B, Suranyi P, Kiss P, Brott BC, Elgavish A, Saab-Ismail NH, Simor T, Elgavish GA: **Gd(ABE-DTTA), a novel contrast agent, at the MRI-effective dose shows absence of deleterious physiological effects in dogs.** *Pharmacology* 2006, **77:**188-194.
79. Friedrich MG, Abdel-Aty H, Taylor A, Schulz-Menger J, Messroghli D, Dietz R: **The salvaged area at risk in reperfused acute myocardial infarction as visualized by cardiovascular magnetic resonance.** *J Am Coll Cardiol* 2008, **51:**1581-1587.
80. Schwitter J, Saeed M, Wendland MF, Derugin N, Canet E, Brasch RC, Higgins CB: **Influence of severity of myocardial injury on distribution of macromolecules: extravascular versus intravascular gadolinium-based magnetic resonance contrast agents.** *Journal of the American College of Cardiology* 1997, **30:**1086-1094.
81. Johnston D, Homma S, Liu P, Weilbaecher D, Rokey R, Brady T, Okada R: **Serial changes in nuclear magnetic resonance relaxation times after myocardial infarction in the rabbit: relationship to water content, severity of ischemia, and histopathology over a six-month period.** *Magn Reson Med* 1988, **8:**363-379.
82. Richard V, Murry CE, Reimer KA: **Healing of myocardial infarcts in dogs. Effects of late reperfusion.** *Circulation* 1995, **92:**1891-1901.
83. Hutchins GM, Bulkley BH: **Infarct expansion versus extension: Two different complications of acute myocardial infarction.** *The American Journal of Cardiology* 1978, **41:**1127-1132.
84. Weisman HF, Healy B: **Myocardial infarct expansion, infarct extension, and reinfarction: Pathophysiologic concepts.** *Progress in Cardiovascular Diseases* 1987, **30:**73-110.
85. Nemes A: **Az érsebészet helyzete Magyarországon. Arteriosclerosis obliterans.** In *Vascularis Medicina.* Edited by Meskó É. Budapest: Therapia Kiadó; 2004: 17-19
86. Pennell DJ, Sechtem UP, Higgins CB, Manning WJ, Pohost GM, Rademakers FE, van Rossum AC, Shaw LJ, Yucel EK: **Clinical indications for cardiovascular magnetic resonance (CMR): Consensus Panel report.** *Eur Heart J* 2004, **25:**1940-1965.
87. Nagel E, Kelle S, Fleck E: **Indikationen für kardiovaskuläre Magnetresonanztomographie.** *Medizinische Klinik* 2005, **100:**219-225.
88. Cerqueira MD, Weissman NJ, Dilsizian V, Jacobs AK, Kaul S, Laskey WK, Pennell DJ, Rumberger JA, Ryan T, Verani MS: **Standardized myocardial segmentation and nomenclature for tomographic imaging of the heart: a statement for healthcare professionals from the Cardiac Imaging Committee of the Council on Clinical Cardiology of the American Heart Association.** *Circulation* 2002, **105:**539-542.
89. Paetsch I, Jahnke C, Wahl A, Gebker R, Neuss M, Fleck E, Nagel E: **Comparison of dobutamine stress magnetic resonance, adenosine stress magnetic resonance, and adenosine stress magnetic resonance perfusion.** *Circulation* 2004, **110:**835-842.
90. Nagel E, Lorenz C, Baer F, Hundley WG, Wilke N, Neubauer S, Sechtem U, van der Wall E, Pettigrew R, de Roos A, et al: **Stress cardiovascular magnetic resonance: consensus panel report.** *J Cardiovasc Magn Reson* 2001, **3:**267-281.

91. Hamdan A, Kelle S, Schnackenburg B, Fleck E, Nagel E: **Improved quantitative assessment of left ventricular volumes using TGrE approach after application of extracellular contrast agent at 3 Tesla.** *J Cardiovasc Magn Reson* 2007, **9:**845-853.
92. Pennell DJ, Underwood SR, Manzara CC, Swanton RH, Walker JM, Ell PJ, Longmore DB: **Magnetic resonance imaging during dobutamine stress in coronary artery disease.** *Am J Cardiol* 1992, **70:**34-40.
93. Baer FM, Voth E, Theissen P, Schneider CA, Schicha H, Sechtem U: **Coronary artery disease: findings with GRE MR imaging and Tc-99m-methoxyisobutyl-isonitrile SPECT during simultaneous dobutamine stress.** *Radiology* 1994, **193:**203-209.
94. van Rugge FP, van der Wall EE, Spanjersberg SJ, de Roos A, Matheijssen NA, Zwinderman AH, van Dijkman PR, Reiber JH, Bruschke AV: **Magnetic resonance imaging during dobutamine stress for detection and localization of coronary artery disease. Quantitative wall motion analysis using a modification of the centerline method.** *Circulation* 1994, **90:**127-138.
95. Nagel E, Lehmkuhl HB, Bocksch W, Klein C, Vogel U, Frantz E, Ellmer A, Dreysse S, Fleck E: **Noninvasive Diagnosis of Ischemia-Induced Wall Motion Abnormalities With the Use of High-Dose Dobutamine Stress MRI : Comparison With Dobutamine Stress Echocardiography.** *Circulation* 1999, **99:**763-770.
96. Hundley WG, Hamilton CA, Thomas MS, Herrington DM, Salido TB, Kitzman DW, Little WC, Link KM: **Utility of fast cine magnetic resonance imaging and display for the detection of myocardial ischemia in patients not well suited for second harmonic stress echocardiography.** *Circulation* 1999, **100:**1697-1702.
97. Wahl A, Paetsch I, Roethemeyer S, Klein C, Fleck E, Nagel E: **High-dose dobutamine-atropine stress cardiovascular MR imaging after coronary revascularization in patients with wall motion abnormalities at rest.** *Radiology* 2004, **233:**210-216.
98. Syed MA, Paterson DI, Ingkanisorn WP, Rhoads KL, Hill J, Cannon RO, 3rd, Arai AE: **Reproducibility and inter-observer variability of dobutamine stress CMR in patients with severe coronary disease: implications for clinical research.** *J Cardiovasc Magn Reson* 2005, **7:**763-768.
99. Lubbers DD, Janssen CH, Kuijpers D, van Dijkman PR, Overbosch J, Willems TP, Oudkerk M: **The additional value of first pass myocardial perfusion imaging during peak dose of dobutamine stress cardiac MRI for the detection of myocardial ischemia.** *Int J Cardiovasc Imaging* 2008, **24:**69-76.
100. Gebker R, Jahnke C, Manka R, Hamdan A, Schnackenburg B, Fleck E, Paetsch I: **Additional value of myocardial perfusion imaging during dobutamine stress magnetic resonance for the assessment of coronary artery disease.** *Circ Cardiovasc Imaging* 2008, **1:**122-130.
101. Wahl A, Paetsch I, Gollesch A, Roethemeyer S, Foell D, Gebker R, Langreck H, Klein C, Fleck E, Nagel E: **Safety and feasibility of high-dose dobutamine-atropine stress cardiovascular magnetic resonance for diagnosis of myocardial ischaemia: experience in 1000 consecutive cases** *Eur Heart J* 2004, **25:**1230-1236.
102. Poldermans D, Fioretti PM, Boersma E, Forster T, van Urk H, Cornel JH, Arnese M, Roelandt RT: **Safety of dobutamine-atropine stress echocardiography in patients with suspected or proven coronary artery disease.** *Am J Cardiol* 1994, **73:**456-459.

103. Picano E, Mathias W, Jr., Pingitore A, Bigi R, Previtali M: **Safety and tolerability of dobutamine-atropine stress echocardiography: a prospective, multicentre study. Echo Dobutamine International Cooperative Study Group.** *Lancet* 1994, **344:**1190-1192.
104. Elhendy A, Mahoney DW, Khandheria BK, Burger K, Pellikka PA: **Prognostic significance of impairment of heart rate response to exercise: Impact of left ventricular function and myocardial ischemia.** *J Am Coll Cardiol* 2003, **42:**823-830.
105. Wellnhofer E, Olariu A, Klein C, Grafe M, Wahl A, Fleck E, Nagel E: **Magnetic resonance low-dose dobutamine test is superior to SCAR quantification for the prediction of functional recovery.** *Circulation* 2004, **109:**2172-2174.
106. Landesberg G, Berlatzky Y, Bocher M, Alcalai R, Anner H, Ganon-Rozental T, Luria MH, Akopnik I, Weissman C, Mosseri M: **A clinical survival score predicts the likelihood to benefit from preoperative thallium scanning and coronary revascularization before major vascular surgery.** *Eur Heart J* 2007, **28:**533-539.

# 9 PUBLICATIONS

## 9.1 Peer reviewed original research publications related to this thesis

1. Kirschner R, Toth L, Varga-Szemes A, Simor T, Suranyi P, Kiss P, Ruzsics B, Toth A, Baker R, Brott B, et al: Differentiation of acute and four-week old myocardial infarct with Gd(ABE-DTTA)-enhanced CMR. *Journal of Cardiovascular Magnetic Resonance* 2010, 12:22. IF: 2.28

2. Kirschner R, Varga-Szemes, A., Simor, T., Suranyi, P., Kiss, P., Ruzsics, B., Brott, BC., Elgavish, A., Elgavish, GA.: Acute infarct selective MRI contrast agent. *Int J Cardiovasc Imaging* 2011 (in press). IF: 2.151

3. Kirschner R, Pécsvárady Z, Bedros RJ, Tóth L, Kiss K, Simor T: Dobutaminterheléses szív mágneses rezonanciás vizsgálat alsó végtagi érszűkületben szenvedő betegeken. *Orv Hetil* 2011, 152:282-291.

## 9.2 Review article publication (peer reviewed) related to this thesis

1. Kirschner R, Tóth L, Simor T: A dobutaminterheléses szív-MR-vizsgálat szerepe a miokardiális iszkémia kimutatásában. *Cardiologia Hungarica* 2011, 41:30-36.

## 9.3 Review article publication related to this thesis

1. Kirschner R, Pecsvarady Zs: The role of MR and CT angiography in the assessment of PAD and cardiovascular status. Hungarian cardiologist, 2006. 1A (supplement)

## 9.4 Citable peer reviewed research presentations/abstracts related to this thesis

1. Kirschner R, Varga-Szemes A, Toth L, Simor T, Suranyi P, Ruzsics B, Kiss P, Toth A, Baker R, Brott BC, Litovsky S, Elgavish A, Elgavish GA.: Reinfarction-specific Magnetic Resonance Imaging Contrast Agent. *Journal of the American College of*

*Cardiology*.55(2010, Supplement 1):A84.E795 A784.E795. Scientific Meeting of the American College of Cardiology, 2010, Atlanta, GA, USA IF: 12.535

2. Kirschner R, Varga-Szemes A, Simor T, Suranyi P, Ruzsics B, Kiss P, Brott BC, Litovsky S, Elgavish A, Elgavish GA.: Acute Infarct Selective Magnetic Resonance Imaging Contrast Agent. *Journal of the American College of Cardiology* T 56: B87-B88 TCT 2010 Congress, Washington DC, USA IF:12.535

3. Kirschner R, Simor T: *Feasibility and safety of Dobutamine stress CMR for cardiac evaluation of patients with PAD*. Will be published in *International Journal of Cardiovascular Imaging*. 39th Annual Meeting of the North American Society for Cardiovascular Imaging, 2011, Baltimore, MD, USA IF:2.151

### 9.5 Peer reviewed research presentations/abstracts related to this thesis

1. Kirschner R, Varga-Szemes A, Simor T, Elgavish GA *Infarct Age Differentiation with Gd(ABE-DTTA) MRI Contrast Agent.* Oral presentation at the Annual Congress of the Hungarian Society of Cardiology, Balatonfüred, Hungary May 12 2011

### 9.6 Original peer reviewed publications not related to this thesis

1. Kirschner R, Varga-Szemes, A., Simor, T., Brott, BC., Litovsky, S., Elgavish, A., Elgavish, GA.: Quantification of Myocardial Viability Distribution with Gd(DTPA) Bolus-Enhanced Signal Intensity-Based Percent Infarct Mapping. *Magnetic Resonance Imaging* 2011 (in press). IF: 2.026

2. Kirschner R, Bodrogi I, Kulhavi C, et al. : K-cell activity in patients with germ cell testicular tumors. Effect of cytostatic therapy. Orv Hetil (Hungary), Mar 15 1992, 133(11)

### 9.7 Citable peer reviewed presentations/abstracts

1. Kirschner R, Varga-Szemes A, Simor T, Suranyi P, Ruzsics B, Kiss P, Brott BC, Litovsky S, Elgavish A, Elgavish GA.: Accurate Determination of Myocardial Viability Distribution with Percent Infarct Mapping. *International Journal of Cardiovascular Imaging (in press).* 38th Annual Meeting of the North American Society for Cardiovascular Imaging, 2010, Seattle, WA, USA IF:2.151

2. Varga-Szemes A, Ruzsics B, Kirschner R, Singh S, Brott BC, Simor T, Elgavish A, Elgavish GA.: Determination of Infarct Size In Ex Vivo Swine Hearts Using Gadolinium-Enhanced Multi-Detector Computed Tomography, *J Cardiovasc Comput Tomogr 2010;4:S71.,* 5th Annual Scientific Meeting of the Society of Cardiovascular Computed Tomography, 2010, Las Vegas, NV, USA

3. Varga-Szemes A, Ruzsics B, Kirschner R, Singh SP, Simor T, Elgavish A, Elgavish G: Gadolinium-Enhanced Multi-Detector Computed Tomography for the Evaluation of Myocardial Infarct. *International Journal of Cardiovascular Imaging (in press).* 38th Annual Meeting of the North American Society for Cardiovascular Imaging, 2010, Seattle, WA, USA IF: 2.151

4. Varga-Szemes A., Kirschner R., Toth L, Brott BC, Simor T, Elgavish A, Elgavish G: In Vivo R1 Based Percent Infarct Mapping Using Continuous Gd(DTPA) Infusion Aided Magnetic Resonance Imaging. *International Journal of Cardiovascular Imaging (in press).* 38th Annual Meeting of the North American Society for Cardiovascular Imaging, 2010, Seattle, WA, USA IF:2.151

5. Kirschner R., Varga-Szemes A., Simor T, Brott BC, Litovsky L, Elgavish A, Elgavish G: Quantification of infarct size and mixing of necrotic and viable myocardial tissue with Signal Intensity-Based Percent Infarct Mapping Imaging. *European Heart Journal (in press).* Congress of the European Society of Cardiology, 2011, Paris IF:9.8

### 9.8 Peer reviewed presentations/abstracts

1. Kirschner R., Balogh S., Sperr E., Szilágyi L., Rónaszéki A.: Circadian, Day-of-week, Monthly and Seasonal Pattern of Myocardial Infarction. Oral presentation at the Annual Congress of the Hungarian Society of Cardiology, Balatonfüred, Hungary May 6 1999

2. Kirschner R., Nagy K., Rónaszéki A.: Severe aortic stenosis in elderly patients. Poster presentation at the Annual Congress of the Hungarian Society of Internal Medicine, Budapest, November 17 2000

3. Kirschner R., Nagy K., Rónaszéki A.: Severe aortic stenosis in elderly patients. Oral presentation at the Annual Congress of the Hungarian Society of Cardiology, Balatonfüred, May 12 2001

4. Nagy K., Kirschner R., Rónaszéki A.: Hemodynamic lessons during headup tilt test sensitized by isoproterenol. Oral presentation at the Annual Congress of the Hungarian Society of Cardiology, Balatonfüred, May 1 2002

5. Kirschner R., Csiffáry B, Greschik I., Rónaszéki A.: Analysis of clinical parameters in dilated cardiomyopathy with permanent atrial fibrillation. Oral presentation at the Annual Congress of the Hungarian Society of Cardiology, Balatonfüred, May 1 2002

6. Kirschner R., Csiffáry B, Greschik I., Rónaszéki A.: Analysis of clinical parameters in dilated cardiomyopathy with permanent atrial fibrillation . Poster presentation at the Annual Congress of the Hungarian Society of Internal Medicine, Budapest, November 11 2002

7. Kirschner R.: The role of MR and CT angiography in PAD and in the assessment of cardiovascular status. Oral presentation at the XVII. Congress of the Society of Physicians of Pest County, April 22 2006

8. Kirschner R.: The role of MR and CT angiography in the assessment of PAD and cardiovascular status. Oral presentation at the Annual Congress of the Hungarian Society of Cardiology, May 11 2006

9. Kirschner R: MR and CT angiography. Oral presentation at the Annual Congress of the Hungarian Society of Young Hypertoniologists, September 09 2006

### 9.9 Additional publications - Selected presentations/abstracts

1. Kirschner R.: role of the angiotensin II receptor blockers in the treatment of hypertension. Oral presentation for internists, June 5 2005

2. Kirschner R : Cardiovascular prevention. Oral presentation at Scientific session in Pulsus Health Center, Budapest, September 21 2004

3. Kirschner R.: The differential diagnostics of the chest pain. Oral presentation at Scientific session in Flór Ferenc Hospital of Pest County, Kistarcsa, January 13 2005

4. Kirschner R: The treatment of hypertension based on international guidelines (JNC VII, ESH/ESC). Oral presentation at Postgraduate educational scientific session at Semmelweis University, 2nd dept. of Internal Medicine, Budapest, September 14 2005

5. Kirschner R.: New therapeutic aspects in lipidology. Oral presentation for internists, Kistarcsa, May 6 2003 6. Kirschner R: More simple, effective and controllable treatment of hypertension. Oral presentation for internists, Godollo, January 4 2006

6. Kirschner R.: The treatment of hypertension with angiotensin II receptor blockers, case studies. Oral presentation for GP-s, Kistarcsa, April 13 2006

7. Kirschner R.: New therapeutic aspects in lipidology. Oral presentation for GP-s Csomor, May 26 2006

8. Kirschner R. : How could we be more effective with lipid lowering therapy? Oral presentation for GP-s, Godollo, June 16 2006

9. Kirschner R.: Primer and secunder cardiovascular prevention, review of international multicenter studies with irbesartan and clopidogrel. Oral presentation for internists, Godollo, September 29 2006

10. Kirschner R.: The Role of the cardiovascular MRI in Cardiology. Oral presentation at Scientific Session of the Club of Cardiology in Pest County, Gödöllő, April 1 2007

11. .Kirschner R., Péter E.: Amyloidosis of the heart and MR diagnostics (case study). Oral presentation at postgrad. educational scientific session Flór Ferenc Hospital of Pest County, Kistarcsa, September 27 2007

12. Kirschner R., Kiss K.: MR diagnostics of the hypertrophical cardiomyopathy (case study). Oral presentation at postgrad. educational scientific session Flór Ferenc Hospital of Pest County, Kistarcsa, February 25 2008

# 10 **ACKNOWLEDGEMENT**

I'm thankful to my family for their love, help, patience, perseverance and empathy.

I wish to acknowledge the support and help to my teachers, friends and associates:

Simor Tamás, MD, PhD
Gabriel A Elgavish, PhD
Rőth Erzsébet, MD, DSc
Varga-Szemes Ákos, MD
Merkely Béla, MD, DSc
Kiss Pál, MD, PhD
Surányi Pál, MD, PhD
Ruzsics Balázs, MD, PhD
Tóth Attila, MD
Tóth Csaba
Silvio Litovsky, MD
Vincent B. Ho, MD, FAHA
Brigitta C. Brott, MD
Pécsvárady Zsolt, MD, PhD
Tóth Levente, MD
Kiss Krisztián, MD
Dezhi Wang, MD